Non-Abelian Anyons: Statistical Repulsion and Topological Quantum Computation

Viktor Qvarfordt

2017-04-21 13:33

Abstract

...

Contents

Chapter 1

Introduction: How anyons arise

?⟨chap:how anyons arise⟩?

It is well known that in three dimensions all particles can be divided into two classes; bosons and fermions. The wave function of multiple identical bosons is symmetric in the particle coordinates while fermions have anti-symmetric wave function,

$$\begin{aligned} \psi(x_1, x_2) &= +\psi(x_2, x_1), \quad \text{for bosons,} \\ \psi(x_1, x_2) &= -\psi(x_2, x_1), \quad \text{for fermions.} \end{aligned} \tag{1.1}$$ {?}

This leads to Bose-Einstein statistics for bosons, and Dirac-Fermi statistics and the Pauli exclusion principle for fermions. The situation is quite different in two spatial dimensions, (clockwise) exchange of two particles can introduce any phase α so that

$$\psi(x_1, x_2) = e^{i\alpha}\psi(x_2, x_1). \tag{1.2}$$ {?}

Since α can take any value, the term "anyon" was coined for such particles, originally by Frank Wilczek [2]. This can be seen as an interpolation between bosons $\alpha = 0$ and fermions $\alpha = \pi$.

More generally the internal degrees of freedom can be higher dimensional, so that (clockwise) exchange of two anyons introduces an arbitrary unitary change U to the wave function

$$\psi(x_1, x_2) = U\psi(x_2, x_1). \tag{1.3}$$ {?}

When U is one dimensional it is on the form $U = e^{i\alpha}$ and we call such anyons abelian, otherwise we call them non-abelian.

1.1 Particle statistics in $n \geq 2$ dimensions

Consider N identical quantum mechanical particles on a spatial manifold M. The configuration space $\mathcal{C}_N$ is the space of possible configurations for the N particles, it is given by

$$\mathcal{C}_n = \frac{M^n - \Delta_n}{S_n}. \tag{1.4}$$ {?}

By removing the set

$$\Delta_n = \{(x_1, \ldots, x_n) \in M^n \mid x_i = x_j \text{ for some } i, j\} \tag{1.5}$$ {?}

of configurations where particles occupy the same point in space, known as a "hard-core" condition, we allow for non-trivial exchange statistics. Without this condition we get bosons. To model the fact that the particles are identical, we form the quotient of $M^n - \Delta_n$ by the symmetric group S_n acting on the coordinates $(x_1, \ldots, x_n)$. In this way all permutations of the n particles are considered to be the same configuration, i.e. $(\ldots, x_j, \ldots, x_k, \ldots) = (\ldots, x_k, \ldots, x_j, \ldots)$ in $\mathcal{C}_N$.

Consider an exchange of particles, that is, take n identical particles on M with given positions and move them around until they are back at some permutation of the original positions. Since the particles are identical, such an exchange is described by a loop in the configuration space $\mathcal{C}_n$. More precisely, a loop $\alpha(t)$ in $\mathcal{C}_n \times [0,1]$, where $t \in [0,1]$ can be considered as the time parameter, corresponds to world-lines of particle trajectories in $M \times [0,1]$. The corresponding world-lines are constructed by choosing a representative of $\alpha(t)$ in $M^n \times [0,1]$ and then projecting the coordinates of each particle into $M \times [0,1]$.

In this way, each loop in $\mathcal{C}_n$ corresponds a classical motion of the particles along world-lines starting and ending in the same configuration. The corresponding quantum mechanical dynamics is obtained by quantizing the system via the path integral formulation [9, 1, 10]. In this way, homotopically equivalent paths can be seen to give the same contribution. Thus, it is really the fundamental group of the configuration space that characterize fundamentally different particle exchanges.

Another way to see that homotopically equivalent paths represent the same physical particle exchange is via the The Aharonov-Bohm effect. Particles in two spatial dimensions can be modeled in three dimensions by charged magnetic flux tubes, as these particles move around each other, they gain a quantum phase due to the Aharonov-Bohm effect, this phase is independent of continuous deformations of the path. For more details on this, see [13, 8].

We shall now see how the fundamental group of the configuration space determines particles statistics.

1.1.1 Exchange of two identical particles in d dimensional Euclidean space

The configuration space of two identical particles (with hard-core condition) in $\mathbb{R}^d$ is given by

$$\mathcal{C} = \frac{(\mathbb{R}^d)^2 - \Delta}{S_2}. \tag{1.6}$$ {?}

The space $(\mathbb{R}^d)^2$ can be factored as $\mathbb{R}^d_{\text{cm}} \times \mathbb{R}^d_{\text{rel}}$ where $\mathbb{R}^d_{\text{cm}}$ gives the coordinates of the center of mass for the two particles and $\mathbb{R}^d_{\text{rel}}$ gives the relative coordinate of the two particles. Let $x_1, x_2 \in \mathbb{R}^d$ be the (absolute) coordinates of the two particles, so that $x = (x_1, x_2) \in \mathcal{C}$. We then define

$$x_{\text{cm}} = \frac{1}{2}(x_1 + x_2), \quad x_{\text{rel}} = \frac{1}{2}(x_1 - x_2). \tag{1.7}$$ {?}

Now, $\Delta = \{(x_1, x_2) \in (\mathbb{R}^d)^2 \mid x_1 = x_2\}$ is precisely the origin of $\mathbb{R}^d_{\text{rel}}$. Furthermore, quotiening with S_2 corresponds to quotiening with the antipodal equivalence relation

$$x \sim y \iff x = -y. \tag{1.8}$$ {?}

Thus we have

$$\mathcal{C} = \mathbb{R}^d_{\text{cm}} \times \underbrace{(\mathbb{R}^d_{\text{rel}} - \{0\})/\sim}_{\mathcal{C}_{\text{rel}}} \tag{1.9}$$ {?}

and we see that the center of mass contributes trivially to the topology of the configuration space, the choice of center of mas can be seen as a gauge freedom.

The topology of the relative configuration space $\mathcal{C}_{\text{rel}}$ can be understood with the following observation. The real projective d-space is the d-sphere with antipodal points identified,

$$\mathbb{RP}^d = S^d/\sim. \tag{1.10}$$ {?}

Furthermore, we have $\mathbb{R}^d - \{0\} \cong \mathbb{R}_+ \times S^{d-1}$ Thus,

$$\begin{aligned} \mathcal{C}_{\text{rel}} &= (\mathbb{R}^d - \{0\})/\sim \\ &\cong (\mathbb{R}_+ \times S^{d-1})/\sim \\ &\cong \mathbb{R}_+ \times S^{d-1}/\sim \\ &\cong \mathbb{R}_+ \times \mathbb{RP}^{d-1}. \end{aligned} \tag{1.11}$$ {?}

Since the fundamental group has the property that $\pi_1(X \times Y) \cong \pi_1(X) \times \pi_1(Y)$ for path connected spaces X and Y we have

$$\pi_1(\mathcal{C}) = \pi_1(\mathbb{RP}^{d-1}) = \begin{cases} \mathbb{Z}, & d = 2 \\ \mathbb{Z}_2, & d \geq 3 \end{cases} \tag{1.12}$$ {?}

as basic result from topology, showing how the case of two spatial dimensions is special.

The space $\mathcal{C}_{\text{rel}}$ can be seen as the half plane $\mathbb{R}^2_{y\geq 0} - \{0\}$ with x and $-x$ identified, or geometrically as a punctured cone.

1.1.2 Exchange of n identical particles in d dimensional Euclidean space

The above example can be generalized to n particles in d dimensional flat space. The corresponding configuration space is then

$$\mathcal{C}_n = \frac{\left(\mathbb{R}^d\right)^n - \Delta_n}{S_n} \tag{1.13}$$ {?}

and the fundamental group of this configuration space is given by [5] as

$$\pi_1(\mathcal{C}_n) = \begin{cases} B_n, & \text{for } d = 2 \\ S_n, & \text{for } d \geq 3 \end{cases} \tag{1.14}$$ {?}

where B_n is the braid group on n strands. This observation motivates the study of anyons in two dimensions. It is the braid group that gives rise to the phenomenon of anyons, thus we begin by studying the braid group.

1.2 The braid group

?⟨sec:braid group⟩?
?⟨eq:braid relations⟩?
The braid group B_n is the group with generators $\sigma_1, \ldots, \sigma_{n-1}$ and relations

$$\sigma_i\sigma_j = \sigma_j\sigma_i \quad \text{if} \quad |i-j| \geq 2, \tag{1.15a}$$

?eq:braid relation 1?

$$\sigma_i\sigma_{i+1}\sigma_i = \sigma_{i+1}\sigma_i\sigma_{i+1}. \tag{1.15b}$$

?eq:braid relation 2?

Note that it has infinitely many elements. The symmetric group S_n is defined as the braid group with the additional relation $\sigma_j^2 = 1$ for all j, it is a finite group. The braid group can be understood as representing braids on n strands, the generator σ_j braids the j:th and $j+1$:th strand clockwise, cf. fig. 1.1. The braid group are thus visualized as in figs. 1.2 and 1.3.

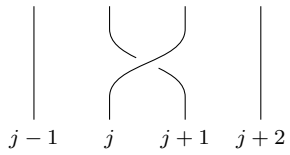

Figure 1.1: Strand representation of the braid group generator σ_j.

g:braid group generators⟩?

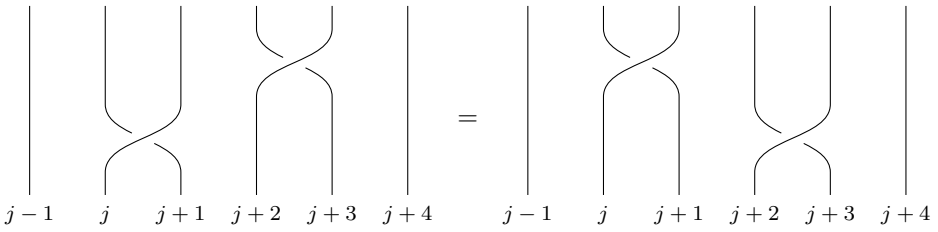

Figure 1.2: Strand representation of $\sigma_j\sigma_{j+2} = \sigma_{j+2}\sigma_j$, illustrating the braid group relation $\sigma_i\sigma_j = \sigma_j\sigma_i$ for $|i-j| \geq 2$ in the case $|i-j| = 2$.

?⟨fig:braid group rel1⟩?

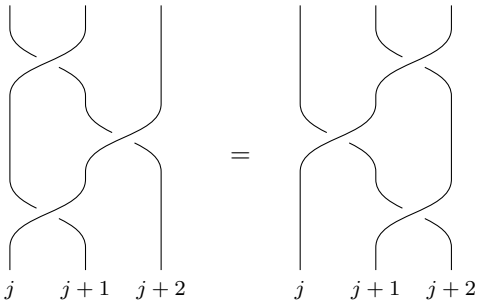

Figure 1.3: Strand representation of the braid group relation $\sigma_j\sigma_{j+1}\sigma_j = \sigma_{j+1}\sigma_j\sigma_{j+1}$.

?⟨fig:braid group rel2⟩?

We now define the braid representing exchange of two strands around p fixed strands, which will play a key role when studying local exclusion of anyons.

Definition 1.2.1. The exchange operator U_p is the braid

$$U_p = \sigma_1\sigma_2\cdots\sigma_p\sigma_{p+1}\sigma_p\cdots\sigma_2\sigma_1, \tag{1.16}$$ {?}

on $p+2$ strands, cf. fig. 1.4, keeping the middle p strands fixed while exchanging the outer strands, 1 and $p+2$, around the middle strands.

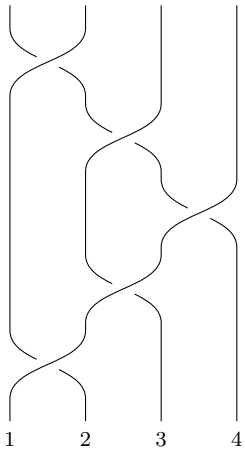

Figure 1.4: Strand representation of the exchange operator $U_2 = \sigma_1\sigma_2\sigma_3\sigma_2\sigma_1$, note how the middle strands, 2 and 3, are kept in place, while the outer strands, 1 and 4, are exchanged.

?⟨fig:Up on strands⟩?

The following observation shall later be useful.

raid generator conjugate⟩?**Lemma 1.2.1.** *All generators of the braid group are conjugate.*

Proof. First, σ_i is conjugate to σ_{i+1} for all i, as seen by

$$\begin{aligned}
(\sigma_i\sigma_{i+1})\sigma_i(\sigma_i\sigma_{i+1})^{-1} &= (\sigma_i\sigma_{i+1}\sigma_i)\sigma_{i+1}^{-1}\sigma_i^{-1} && (1.17)\ \{?\}\\
[\text{eq. (1.15b)}] &= (\sigma_{i+1}\sigma_i\sigma_{i+1})\sigma_{i+1}^{-1}\sigma_i^{-1} && (1.18)\ \{?\}\\
&= \sigma_{i+1}\sigma_i\sigma_i^{-1} && (1.19)\ \{?\}\\
&= \sigma_{i+1}. && (1.20)\ \{?\}
\end{aligned}$$

Finally, conjugation is transitive, thus all braid generators are conjugate. □

Since time evolution of a quantum state is described by unitary operators, we shall be interested in unitary representations of the braid group.

A unitary representation of B_n is a map

$$\begin{aligned}
\rho : B_n &\to U(n)\\
\sigma_j &\mapsto \rho(\sigma_j)
\end{aligned} \tag{1.21}$$ {?}

where $U(n)$ is the group of $n \times n$ unitary matrices over $\mathbb{C}$.

Lemma 1.2.2. *Abelian representations of B_n, i.e. representations on $U(1)$ are such that*

$$\rho(\sigma_j) = e^{i\alpha} \tag{1.22}$$ {?}

for all j.

Proof. $U(1)$ is an abelian group, thus the second braid group relation eq. (1.15b) gives $\sigma_j = \sigma_{j+1}$ for all j. The first braid group relation eq. (1.15a) is trivially satisfied. The elements of $U(1)$ are of the form $e^{i\alpha}$. □

Particles obeying statistics described by abelian representations of the braid group are called abelian anyons.

Corollary 1.2.3. *Since the symmetric group S_n has the additional relation $\sigma_j^2 = 1$ we see that abelian representations of S_n are such that $\rho(\sigma_j) = 1$ for all j or $\rho(\sigma_j) = -1$ for all j, corresponding to bosons and fermions, respectively.*

Higher dimensional representations of the braid group are representations on $U(n)$ for $n \geq 2$, such representations are generally non-abelian. In this thesis we shall primarily be concerned with non-abelian anyons, i.e. anyons obeying statistics described by non-abelian representations of the braid group. For a general discussion of the non-abelian representation theory of braid groups, see [7]. It is in general difficult to characterize the non-abelian representations, it is furthermore not always clear whether a given representation corresponds to a physically realizable particles. In this thesis we shall therefore use a general framework of abstract anyon models rooted in quantum field theory to characterize possible non-abelian representations and study the dynamics of such anyons.

Higher-dimensional representations of S_n also exist, such particles are sometimes called plektons and their statistics known as parastatistics. However, it has been shown that parastatistics in $d \geq 3$ dimensions can always be reduced to bosons or fermions by introducing additional internal degrees of freedom [5]. However, in $d = 2$ dimensions parastatistics cannot be reduced, suggesting that anyons in two dimensions are fundamentally different from particles in $d \geq 3$ dimensions.

1.3 Measuring quantum phases

global vs relative phase⟩?

Everything that can be measured in quantum mechanics is represented by self-adjoint operators, called observables. The result of a measurement is one of the eigenvalues of the observable. If $|\psi\rangle$ is the quantum state being measured, then the expectation of the measurement is

$$\langle\psi|A|\psi\rangle. \tag{1.23}$$ {?}

The two quantum states $|\psi\rangle$ and $e^{i\varphi}|\psi\rangle$ represent the same physical state. The phase φ of the second state is not physical, it cannot be measured since

$$\langle e^{i\varphi}\psi|A|e^{i\varphi}\psi\rangle = e^{-i\varphi}e^{i\varphi}\langle\psi|A|\psi\rangle = \langle\psi|A|\psi\rangle. \tag{1.24}$$ {?}

Such a phase is called a global phase.

A relative phase is a phase "between" two states, which can be measured. Consider an orthonormal basis $\{|0\rangle, |1\rangle\}$ and the general state

$$|\psi\rangle = ae^{i\alpha}|0\rangle + be^{i\beta}|1\rangle. \tag{1.25}$$ {?}

For a general (Hermitian) observable A, the expectation of a measurement is

$$\begin{aligned}\langle\psi|A|\psi\rangle &= \begin{pmatrix} ae^{-i\alpha} & be^{-i\beta}\end{pmatrix}\begin{pmatrix} A_{00} & A_{01}\\ A_{10} & A_{11}\end{pmatrix}\begin{pmatrix} ae^{-i\alpha}\\ ae^{-i\beta}\end{pmatrix}\\ &= a^2A_{00} + b^2A_{11} + ab\left(A_{01}e^{i(\beta-\alpha)} + A_{10}e^{i(\alpha-\beta)}\right)\\ &= a^2A_{00} + b^2A_{11} + 2ab\,\mathrm{Re}\left(A_{01}e^{i(\beta-\alpha)}\right).\end{aligned} \tag{1.26}\{?\}$$

The relative phase is $\beta-\alpha$ and the above shows that it affects measurements for observables with off-diagonal elements, this can be understood as interference. Note that the phases α and β can be seen as global phases of $|0\rangle$ and $|1\rangle$, explaining why neither can be directly measured.

Similarly, if we have two copies of a given state $|\psi\rangle$, then perform an operation on one of them so that $|\psi\rangle \mapsto e^{i\varphi}|\psi\rangle$, the introduced phase φ can be measured by forming a state where it is the relative phase. Indeed, consider the product state

$$|\Psi\rangle = \frac{1}{\sqrt{2}}\Big(|\psi\rangle\otimes|0\rangle + e^{i\varphi}|\psi\rangle\otimes|1\rangle\Big) \tag{1.27}\{?\}$$

where $|0\rangle$ and $|1\rangle$ are two orthonormal states. Now, perform the Hadamard transform eq. (6.16),

$$H|\Psi\rangle = \frac{1}{2}\Big(\left(1+e^{i\varphi}\right)|\psi\rangle\otimes|0\rangle + \left(1-e^{i\varphi}\right)|\psi\rangle\otimes|1\rangle\Big) \tag{1.28}\{?\}$$

and perform a measurement in the $\{|0\rangle,|1\rangle\}$ space. The probability of finding $|\Psi\rangle$ in the state $|0\rangle$ is

$$\begin{aligned}\left|\frac{1+e^{i\varphi}}{2}\right|^2 &= \frac{1}{4}\left(1+e^{i\varphi}\right)\left(1+e^{i\varphi}\right)^*\\ &= \frac{1}{4}\left(1+e^{i\varphi}e^{-i\varphi}+e^{i\varphi}+e^{-i\varphi}\right)\\ &= \frac{1}{4}\left(2+2\cos(\varphi)\right)\\ &= \frac{1}{2}\left(1+\cos(\varphi)\right),\end{aligned} \tag{1.29}\{?\}$$

which clearly depends on φ.

This scheme can in principle be used to measure the anyonic phase. In practice, special interferometry can be used to observe the anyonic phase, this is discussed in [13]. Note that as one anyon is exchanged around one or several other anyons, the introduced phase can only be measured after one full loop as been traversed and the phase can be compared to another anyon. Thus, it is not physical to say that the phase continuously (or in any other way) increases during the exchange. That is, how phase is affected before the particles meet is non-physical, we are free to choose this so long as the choice respects the result of a complete winding of particles; this illustrates the gauge invariance of the anyonic phase during braiding.

1.4 Anyon models and realizability

models and realizability⟩? This text focuses on the mathematical aspects of anyons, however, in this section we give a short account of possible physical realizations for anyons. This topic

is is further discussed in for instance [20, 21, 30].

Abelian anyons have been claimed to detected in the fractional quantum hall (FQH) effect. [35] Furthermore, it has been conjectured that non-abelian anyons can be realized in FQH liquids at the filling fractions $\nu = 5/2$, where Ising anyons are thought to exist [33]. Partial experimental results exist which support the existence of non-abelian anyons [36]. The Fibonacci anyon model with is studied in chapter 5 has support from the topological quantum field theory Chern-Simons-Witten (CSW).

There are different attempts to identify if particles obey anyonic statistics. Interferometry methods have been developed, as in [13]. Another approach is to study the wave function density, as outlined in [**?**].

In the literature one generally encounters two types of anyons.

1. Anyons with quantum dynamics, giving rise to anyonic particle statistics. Such particles must necessarily be allowed to move freely in space, such as in a gas. This is the type of anyons that one has in mind when discussion statistical repulsion.

2. Anyons with fixed or controlled coordinates. This is the type of anyons that one has in mind when discussing the use of anyons for topological quantum computation. The anyons need to be fixed so that controlled braiding can be performed. In principle this can be achieved by forcing the position of the anyons by placing each anyon in a deep potential that can be externally controlled.

Chapter 2

Statistical repulsion of anyons

ap:statistical repulsion⟩? Omarbetas.

Chapter 3

Abstract anyon models

?⟨anyon models⟩? In this chapter we shall present the framework of abstract anyon models, leading up to the succeeding chapter that characterizes braiding of anyons described abstract anyon models.

Anyon models can be modeled by unitary braided tensor categories, see [11, appendix E] and [17, 18, 19, 16]. However, setting up this framework in full generality is redundant for our purposes and we take a more straight forward approach, which is also most common in the literature. The benefit of the categorical approach is that consistency of braiding and fusion is most naturally shown this way. We shall see the ties between the straight forward approach and the categorical model in when discussing the consistency conditions in section 3.6.

This chapter is in part based on [12, 11, 13]. We shall be using the notation that is standard in the literature, and when possible make use of and extend the fusion diagram notation, which greatly clarifies braiding of fusion states.

Starting with section 4.2 we show how a given abstract anyon model gives rise to representations of the braid group.

3.1 Preliminaries

An abstract anyon model consists of a set of labels representing different types of anyons. These labels are known as anyonic charge, topological charge or superselection labels. Anyons can be combined, or fused, to give an anyon of some charge, possibly in different ways. This is modeled by a fusion algebra

$$a \times b = \sum_c N_{ab}^c c \tag{3.1}$$ {?}

representing the possible outcomes from fusion of anyons of type a and b. The fusion multiplicities N_{ab}^c are non-negative integers denoting the number of distinct ways a and b can fuse to c. In each anyon model there is the trivial label 1, representing the vacuum, with the property $N_{a1}^b = N_{1a}^b = \delta_{ab}$, i.e. 1 fuses trivially with every other charge. Furthermore, to each charge a there is a corresponding conjugate charge $\bar{a}$ representing the antiparticle of a, with the property $N_{ab}^1 = \delta_{b\bar{a}}$, i.e. a fuses to the vacuum only with its antiparticle.

The N_{ab}^c distinguishable ways in which a and b can fuse to c can be regarded as an orthonormal basis of a Hilbert space V_{ab}^c. This is the state space, or fusion space, of anyons of type c resulting from fusion of a and b. The states of V_{ab}^c are called fusion states and we denote the basis for V_{ab}^c by

$$\{|ab; c, \mu\rangle, \quad \mu = 1, 2, \ldots, N_{ab}^c\} \tag{3.2}$$ {?}

where $|ab; c, \mu\rangle$ represents the μ:th way in which a and b can fuse to c. This is the notation used by [12].

The splitting space V_c^{ab} is the dual space of the fusion space V_{ab}^c, it is the state space of particles with anyonic charge a and b that can be split from an anyon of charge c.

More generally, the fusion space of anyons of type c resulting from fusion of anyons of type $a_1, \ldots, a_n$ is denoted by $V_{a_1 a_2 \cdots a_n}^c$. This space has a canonical decomposition

$$V_{a_1 a_2 \cdots a_n}^c \cong \bigoplus_{b_1, b_2, \ldots, b_{n-2}} V_{a_1 a_2}^{b_1} \otimes V_{b_1 a_3}^{b_2} \otimes V_{b_2 a_4}^{b_3} \ldots \otimes V_{b_{n-2} a_n}^c \tag{3.3}$$ {?}

with an associated canonical orthonormal basis with elements being the fusion states

$$|a_1 a_2; b_1, \mu_1\rangle \otimes |b_1 a_3; b_2, \mu_2\rangle \otimes \cdots \otimes |b_{n-3} a_{n-1}; b_{n-2}, \mu_{n-2}\rangle \otimes |b_{n-2} a_n; c, \mu_{n-1}\rangle \tag{3.4}$$ {?}

for all possible b_j and μ_j. For convenience we write $b_0 = a_1$ and $b_{-1} = 1$.

Many anyon models of interest have the property that $N_{ab}^c \leq 1$ for all particle types a, b and c. When this is the case, such as for the Fibonacci anyons that we shall consider in chapter 5, the multiplicity label μ can be ignored. This makes the model easier to handle, and we introduce the fusion diagram notation.

3.2 Fusion diagrams

In the previous section we defined

$$|ab; c, \mu\rangle \tag{3.5}$$ {?}

to represent the μ:th way in with a and b fuse to c. It shall be very convenient to use a diagrammatic notation for fusion states when considering braiding of anyons, as we shall see in the following sections. Thus, we introduce the notation

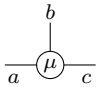

$$\coloneqq |ab; c; \mu\rangle \tag{3.6}$$ {?}

Note that the diagram should be read left/top to right/bottom, i.e. a fuses with b resulting in c. For simplicity we suppress the multiplicity label μ in the notation and write

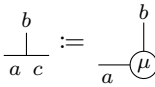

$$\coloneqq |ab; c; \mu\rangle. \tag{3.7}$$ {?}

This is convenient, since most models we shall consider are such that the fusion multiplicities are trivial, $N_{ab}^c \leq 1$. That is, if fusion of a and b to c is possible,

this happens in exactly one way. Then, the multiplicity label μ in $|ab;c,\mu\rangle$ can be ignored, because the only possibility is $\mu = 1$, if $\mu = 0$ the state is not valid. This is not a major simplification in the notation, it shall always be straight forward to add back the multiplicity labels if needed.

The diagram notation is primarily useful when considering fusion of several anyons and extends in a natural way;

(3.8) {?}

denotes fusion of a, b, c to d such that a fuses with b resulting in the intermediate charge e, finally e fuses with c to give the resulting charge d.

The canonical basis for the fusion space $V^c_{a_1 a_2 \cdots a_n}$ with canonical decomposition

$$V^c_{a_1 \cdots a_n} \cong \bigoplus_{b_1, b_2, \ldots, b_{n-2}} V^{b_1}_{a_1 a_2} \otimes V^{b_2}_{b_1 a_3} \otimes V^{b_3}_{b_2 a_4} \ldots \otimes V^c_{b_{n-2} a_n} \tag{3.9}$$ {?}

can thus be written in terms of fusion diagrams, assuming trivial fusion multiplicities, as

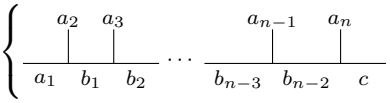

(3.10) {?}

It is thus clear that for given anyons $a_1, \ldots, a_n$ the fusion states are really determined by the intermediate charges b_j.

The real advantage of writing fusions states with fusion diagrams is that braiding is much easier to represent. This will be extremely useful now as we proceed in developing the abstract model for anyons, and characterize braiding.

Consider an arbitrary fusion state $|\psi\rangle = \sum_k c_k |k\rangle$ where $|k\rangle$ denotes the k:th basis fusion states. Let A be a linear operator on the fusion space. The basis fusion states are transformed according to

$$A|k\rangle = \sum_j A_{jk} |j\rangle \tag{3.11}$$?eq:linear op on basis sta

The action of a linear operator A acting on $|\psi\rangle$ is then given by

$$A|\psi\rangle = \sum_k c_k A|k\rangle = \sum_k c_k \sum_j A_{jk}|j\rangle = \sum_j \sum_k c_k A_{jk}|j\rangle. \tag{3.12}$$ {?}

Alternatively, written in Dirac notation, using the resolution of identity $I = \sum_j |j\rangle\langle j|$, we have

$$A|\psi\rangle = \sum_{j,k} |j\rangle \underbrace{\langle j|A|k\rangle}_{A_{jk}} \underbrace{\langle k|\psi\rangle}_{c_k} \tag{3.13}$$ {?}

In what follows, we shall define some important linear operators on fusion spaces. We shall define the operators in terms of their action on the on the standard fusion states, as in eq. (3.11).

3.3 The F operator: Associativity of fusion

The result of fusing multiple anyons must be independent of which anyons are fused first. That is, fusion is associative,

$$(a \times b) \times c = a \times (b \times c) \tag{3.14}$$ {?}

This gives rise to a natural isomorphism between the two decompositions of the fusion space

$$V_{abc}^{d} \cong \bigoplus_{f} V_{ab}^{f} \otimes V_{fc}^{d} \cong \bigoplus_{e} V_{bc}^{e} \otimes V_{ae}^{d}. \tag{3.15}$$ {?}

The first decomposition should be understood as first fusing a with b in all possible ways giving an intermediate charge f, followed by fusing c with f to give the final charge d. The second decomposition should be understood as first fusing b with c in all possible ways giving an intermediate charge e, followed by fusing a with e to give the final charge d.

The first of these two decompositions is referred to as the standard decomposition and the second is the fusion decomposition. We denote this isomorphism by

$$F : \bigoplus_{f} V_{ab}^{f} \otimes V_{fc}^{d} \to \bigoplus_{e} V_{bc}^{e} \otimes V_{ae}^{d} \tag{3.16}$$ {?}

and it can be represented by the F matrix.

Definition 3.3.1. The F matrix F_{abc}^{c} is given by

$$F : \begin{array}{c} b\ \ c \\ |\ \ | \\ a\ e\ d \end{array} \mapsto \begin{array}{c} b\ \ c \\ \smile \\ e \\ |\ \ \\ a\ \ d \end{array} = \sum_{f} \left(F_{abc}^{d}\right)_{fe} \begin{array}{c} b\ \ c \\ |\ \ | \\ a\ f\ d \end{array}. \tag{3.17}$$?F-matrix?

That is, the F-matrix is the change of basis matrix from the standard basis to the fused basis in the fusion space V_{abc}^{d}.

?⟨rem:sum index range⟩? *Remark* 3.3.1 (Implicit range for the index of summation). In eq. (3.17) the summation index f implicitly ranges over all possible labels in the given anyon model, with the obvious restriction that the corresponding fusion state in the summand is valid. That is, the summation index f must be such that

$$\begin{aligned} a \times b &= f \\ f \times c &= d. \end{aligned} \tag{3.18}$$ {?}

Similarly, the label e is restricted so that

$$\begin{aligned} b \times c &= e \\ a \times e &= d. \end{aligned} \tag{3.19}$$ {?}

In what follows we shall let the summation index be implicit in all sums with fusion states as summands.

The following lemma will be useful when computing the F-matrix.

?⟨res:F1⟩? **Lemma 3.3.1.** *Consider the fusion space V^d_{abc}, when one of the particle types is trivial, i.e. a, b, c or d equals 1, then $\dim V^d_{abc} = 1$ and the corresponding F-matrix F^d_{abc} is trivial. More explicitly we have*

$$\begin{aligned} F^d_{1bc} &= \left(F^d_{1bc}\right)_{bd} = 1, \\ F^d_{a1c} &= \left(F^d_{a1c}\right)_{ac} = 1, \\ F^d_{ab1} &= \left(F^d_{ab1}\right)_{db} = 1, \\ F^1_{abc} &= \left(F^1_{abc}\right)_{\overline{c}\,\overline{a}} = 1. \end{aligned} \tag{3.20}$$ {?}

Proof. With $a = 1$ we have, by definition of the F-matrix,

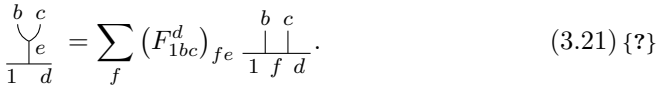

(3.21) {?}

From the fusion diagram on the right hand side we read out $1 \times b = f$ from the first fusion, this is valid only for $f = b$. Similarly, on the left hand side the final fusion reads $1 \times e = d$, implying $e = d$. Since the indices e and f are forced, this implicitly shows that the corresponding fusion spaces is one-dimensional. The other results follow analogously,

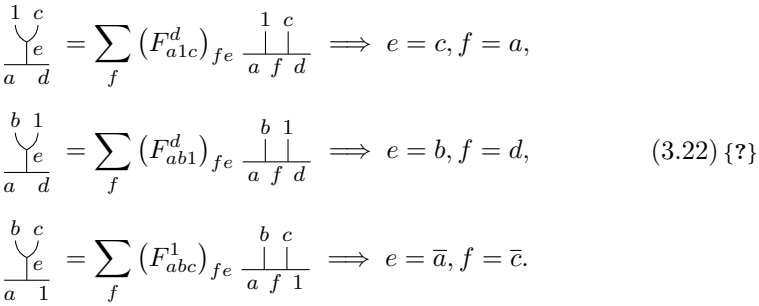

(3.22) {?}

The result can also be realized by noting that three anyons of type a, b and c, where one of them is the trivial type 1, is uniquely determined by their total charge. Indeed, these three anyons are really just two, since the trivial particle 1 fuses trivially, it can be added or removed in the representation without changing anything. Thus, the corresponding F matrix must be trivial in this case. This is particularly clear if b or c equals 1, we then have

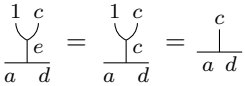

(3.23) {?}

and it is clear that no fusion can occur. □

3.4 The R operator: Commutativity of fusion

The result of fusing a with b must be the same as fusing b with a. That is, fusion is commutative,

$$a \times b = b \times a. \tag{3.24}$$ {?}

This gives rise to a natural isomorphism

$$R : V_{ba}^{c} \to V_{ab}^{c} \tag{3.25}$$ {?}

between the corresponding fusion spaces which can be represented by a unitary matrix R_{ab}^{c} acting on the fused basis states

. (3.26) {?}

Definition 3.4.1. The R matrix R_{ab} is given by

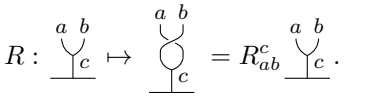

. (3.27) ?R-matrix?

It is clear that R-matrix R_{ab} is diagonal and we can denote this as

$$(R_{ab})_{ij} = \delta_{ij} R_{ab}^{i}. \tag{3.28}$$ {?}

3.5 The B operator: Braiding of standard fusion states

We shall now consider braiding on the standard fusion states. This can be realized by applying the F-matrix to put the state in a basis where the R matrix can be applied immediately, followed by reverting back to the standard basis via F^{-1}. That is, using the F and R-matrix we obtain the relation

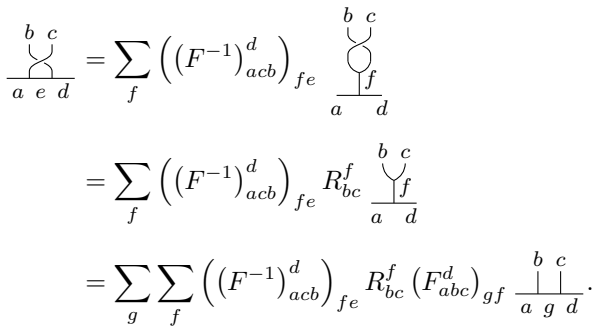

(3.29) {?}

Recall the implicit summation index convention described in remark 3.3.1. From this we define the B-matrix.

?⟨def:B⟩? **Definition 3.5.1.** The B matrix B_{abc}^{d} is given by

$$\left(B_{abc}^{d}\right)_{eg} = \sum_{f} \left(\left(F^{-1}\right)_{acb}^{d}\right)_{ef} R_{bc}^{f} \left(F_{abc}^{d}\right)_{fg}. \tag{3.30}$$ {?}

Symbolically we write this as

$$B = F^{-1} R F. \tag{3.31}$$ {?}

To sum up, the B-matrix braids the standard fusion states according to

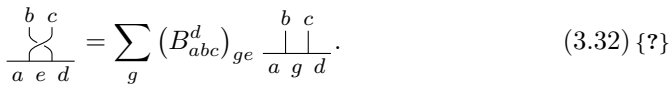

$$= \sum_g \left(B^d_{abc}\right)_{ge} \qquad (3.32)\ \{?\}$$

As a consequence of the definition of the B-matrix and lemma 3.3.1 we have the following lemma, which will be useful when computing the B-matrix.

?⟨res:B1⟩? **Lemma 3.5.1.** *Consider the fusion space V^d_{abc}, when one of the particle types is trivial, i.e. a, b, c or d equals 1, then $\dim V^d_{abc} = 1$ and the corresponding B-matrix B^d_{abc} is one-dimensional,*

$$\begin{aligned} B^d_{1bc} &= \left(B^d_{1bc}\right)_{bc} = R^d_{bc}, \\ B^d_{a1c} &= \left(B^d_{a1c}\right)_{ad} = R^c_{1c} = 1, \\ B^d_{ab1} &= \left(B^d_{ab1}\right)_{da} = R^b_{b1} = 1, \\ B^1_{abc} &= \left(B^1_{abc}\right)_{\overline{c}\,\overline{b}} = R^{\overline{a}}_{bc}. \end{aligned} \qquad (3.33)\ \{?\}$$

3.6 The pentagon and hexagon equations

?⟨sec:pentagon hexagon⟩? When considering an anyon model, it is ultimately the B operator (braid operator) that describes how braiding affects the anyons. The B operator gives the phase change introduced when braiding anyons. In the next chapter we shall explicitly see how the B operator is used to characterize the braid group representation for anyon models. It is the braid group representation that is the relevant property both for the study the dynamics of anyons, but also for developing methods for quantum computation with anyons, known as topological quantum computation.

We have seen that the B-matrix is computed from the F and R-matrices. These matrices are in turn determined by what is known as the pentagon equation

$$\left(F^5_{12c}\right)^d_a \left(F^5_{a34}\right)^c_b = \left(F^d_{234}\right)^c_c \left(F^5_{1e4}\right)^d_b \left(F^b_{123}\right)^e_a \qquad (3.34)\ \text{?eq:pentagon?}$$

and hexagon equation

$$R^g_{ac} \left(F^d_{bac}\right)^g_e R^e_{ab} = \sum_f \left(F^d_{bca}\right)^g_f R^d_{af} \left(F^d_{abc}\right)^f_e . \qquad (3.35)\ \text{?eq:hexagon?}$$

In these equations, all indices are taken as arbitrary particle labels.

These equations should be understood as coherence conditions for fusion and braiding. The diagrammatic version of these equations, found as commutative diagrams in figs. 3.1 and 3.4 and figs. 3.2 and 3.4 make the point clear, and shows that these equations are commutativity constraints for fusion and braiding. Indeed, the pentagon equation is the formal constraint for associativity of fusion,

$$(a \times b) \times c = a \times (b \times c). \qquad (3.36)\ \{?\}$$

As previously hinted, anyon models can be described by braided tensor categories. In this setting, the pentagon and hexagon equations are precisely Mac Lane's coherence theorem [15], showing that no further conditions are required for consistent fusion and braiding. Further details can be found in [11, 12].

Solving the pentagon and hexagon equations is in general highly non-trivial. The equations are multivariate polynomial equations and require elaborate techniques to be solved. First one must fix the gauge freedom that comes from the choice of basis for the fusion space, next an appropriate Gröbner basis can be used to solve the system. See [13] for more details on this approach.

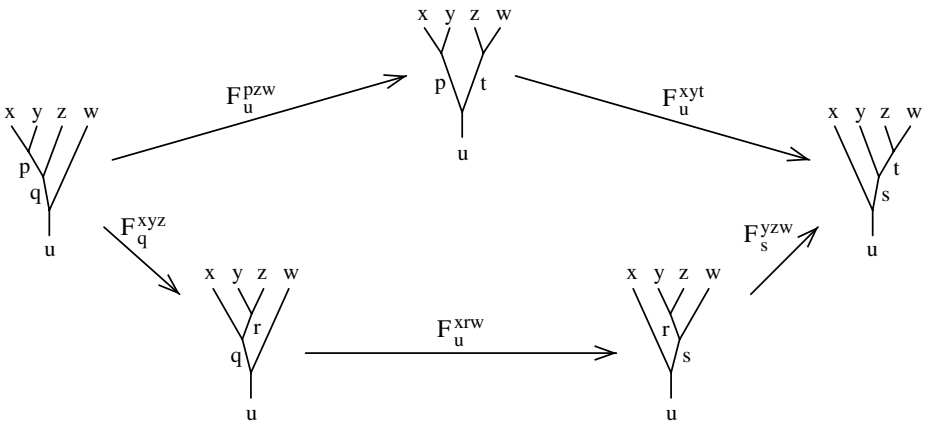

Figure 3.1: The pentagon equation in terms of fusion diagrams. Figure take from [11]. Note that the F-matrix have super- and sub-scripts reversed.

?⟨fig:pentagon_diagram⟩?

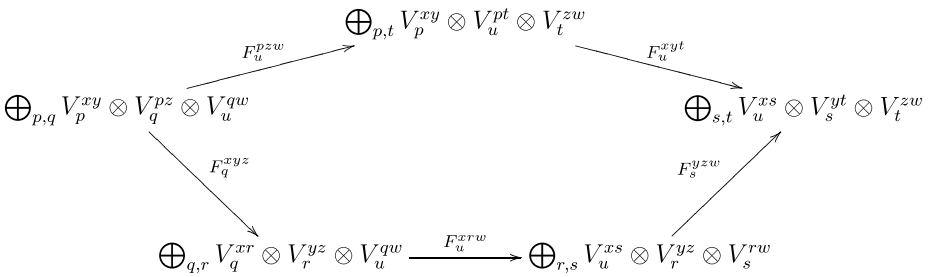

Figure 3.2: The pentagon equation in terms of fusion spaces. Figure take from [11]. Note that the fusion spaces and the F-matrix have super- and sub-scripts reversed.

?⟨fig:pentagon_space⟩?

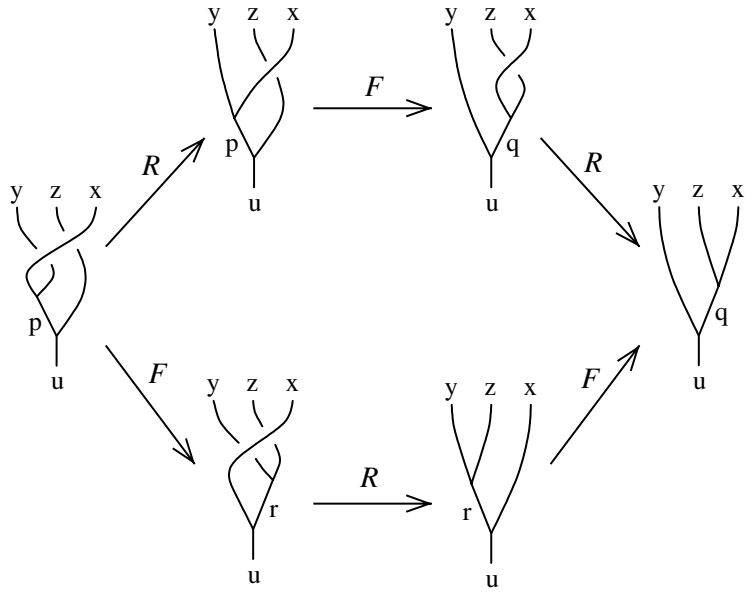

Figure 3.3: The hexagon equation in terms of fusion diagrams. Figure take from [11].

?⟨fig:hexagon_diagram⟩?

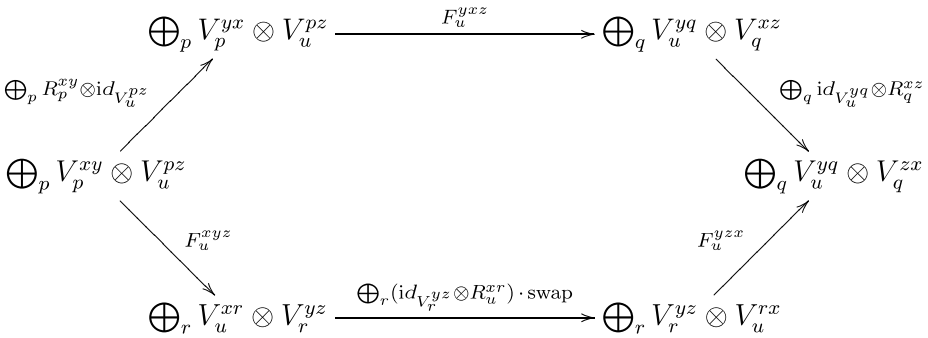

Figure 3.4: The hexagon equation in terms of fusion spaces. Figure take from [11]. Note that the fusion spaces, F-matrix and R-matrix have super- and subscripts reversed.

?⟨fig:hexagon_space⟩?

Chapter 4

Anyonic braid group representations

In this chapter we show how a given anyon model gives rise to representations of the braid group. In particular, a general characterization of the exchange operator U_p is derived. We begin by defining charge sectors of fusion spaces.

4.1 Charge sectors

?⟨sec:charge sectors⟩? Consider any abstract anyon model with a non-trivial particle label t. When considering braiding of two intermediate t anyons in $V_{t^n}^1$, it suffices to work with the basis of $V_{t^n}^1$ restricted to the intermediate charge labels a, b and c in

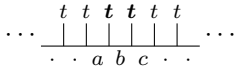

(4.1) {?}

The reason for this is that only these labels are part of the B matrix describing braiding of the two t anyons. Note that we cannot make any assumptions for the charge c, it is not forced to be 1 since we are considering intermediate anyons in the fusion space, only the total charge of the fusion space is specified, in this case 1. The different possible values for c is referred to as different right charge sector. Similarly, also the charge a is unknown, because we are not considering the leftmost particle in the basis, there are really more anyons to the left, that fuse to different resulting charges a. This results in different left charge sectors.

If we fix the both the left and right charge sectors to be trivial, we are really considering braiding of

(4.2) {?}

in $V_{t^2}^1$. This is a different fusion space, with much smaller dimension than $V_{t^n}^1$. There is just one free intermediate charge label here, compared to three free charge labels when not fixing the charge sectors.

Note that having trivial total charge, as in $V_{t^n}^1$, represents the fact that we have exactly n anyons of type t. If the total charge would be t, there would really be $n + 1$ anyons of type t available.

Since we seek to characterize general braiding in $V_{t^n}^1$, including intermediate anyons where both the left and right charge sector are unfixed, we introduce the following definition for convenience.

?⟨def:full fusion space⟩?

Definition 4.1.1. The fusion space $\widetilde{V}_{t^n}$ has basis elements on the form

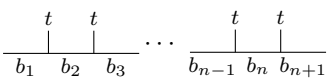

(4.3) {?}

where the charge labels $b_1, b_2, \ldots, b_{n+1}$ range over all values allowed by the fusion rules. The space $\widetilde{V}_{t^n}$ should be thought of as the space $V_{t^n}^1$ but including all possible left and right charge sectors. That is, the space of n anyons of type t with unfixed charge sectors.

The following new notation shall be convenient when working with such fusion spaces.

Definition 4.1.2. The basis fusion states of the fusion space $\widetilde{V}_{t^n}$ are denoted

$$|b_1 b_2 \cdots b_n b_{n+1}\rangle \coloneqq$$

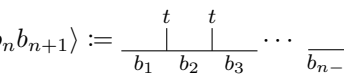

, (4.4) {?}

where the n anyons of type t are implicit in this notation.

Remark 4.1.1. We now have three slightly different notations for fusion spaces, to sum up:

$$V_{t^n}^1 := \text{span}\left\{ \text{fusion tree: } \mathbf{1}, t, b_1, \ldots, b_{n-3}, b_{n-2}, \mathbf{1} \;:\; \text{for all possible } b_j \right\}$$

$$V_{t^n} := \text{span}\left\{ \text{fusion tree: } \mathbf{1}, t, b_1, \ldots, b_{n-3}, b_{n-2}, \boldsymbol{b_{n-1}} \;:\; \text{for all possible } b_j \right\} \quad (4.5)\ \{?\}$$

$$\widetilde{V}_{t^n} := \text{span}\left\{ \text{fusion tree: } \boldsymbol{b_1}, b_2, b_3, \ldots, b_{n-1}, b_n, \boldsymbol{b_{n+1}} \;:\; \text{for all possible } b_j \right\}$$

Note how the only thing that differs are the left and right charge sectors.

We shall now see how braid group representations arise in the fusion space $\widetilde{V}_{t^n}$ for given non-trivial anyonic charge t. We let the left and right charge sectors be unspecified, meaning that the n anyons we consider may really be part of a larger ensemble of anyons. If we in total had exactly n anyons, it would suffice to consider the fusion space $V_{t^n}^1$, i.e. with left and right charge sectors fixed to 1, but we proceed without this restriction. Note that we could instead consider the more general fusion space $\widetilde{V}_{a_1 \cdots a_n}$, however one is most often interested in braiding of anyons of the same type. This is also exactly what we need for the purposes outlined in chapter 2. The fusion space $\widetilde{V}_{a_1 \cdots a_n}$ is in principle treated analogously to $\widetilde{V}_{t^n}$, but the dependence on the different charge labels $a_1, \ldots, a_n$ make the computations more involved.

4.2 Braid group representations in $\widetilde{V}_{t^n}$

ntations in fusion space⟩? Each anyon model gives rise to representations of the braid group, the representations depend on the number of considered anyons and the possible charges sectors. In this and the following sections we give a detailed account of how braid group representations comes about in the framework of abstract anyon models. An account of the general theory of braid group representations, not necessarily arising from abstract anyon models, can be found in [7].

Single out a non-trivial anyonic charge and consider the fusion space $\widetilde{V}_{t^n}$ with the standard basis. In this space we naturally have $n-1$ braid group generators by exchanging neighbouring t anyons, we introduce the following notation.

?⟨def:rho_n sigma_j⟩? **Definition 4.2.1.** The representation of the j:th braid group generator σ_j in $\widetilde{V}_{t^n}$ is denoted $\rho_n(\sigma_j)$.

For example, we have

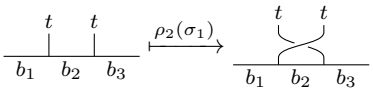

(4.6) {?}

this is precisely the B operator

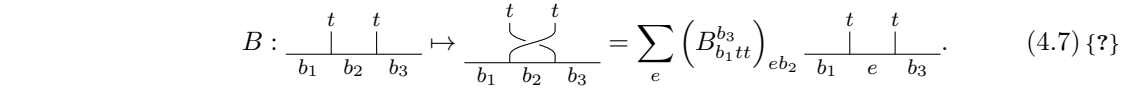

$$= \sum_e \left(B^{b_3}_{b_1tt}\right)_{eb_2}. \tag{4.7}$$ {?}

This shows that $\rho_2(\sigma_1)$ in $\widetilde{V}_{t^2}$ for fixed b_1 and b_3 is given by

$$\rho_2(\sigma_1) = B^{b_3}_{b_1tt}. \tag{4.8}$$ {?}

Thus, in the full basis that is

$$\rho_2(\sigma_1) = \bigoplus_{b_1,b_3} B^{b_3}_{b_1tt}. \tag{4.9}$$ {?}

Indeed, there is no mixing of the values for b_1 or b_3, as seen from the definition of the B matrix, this matrix really only acts on the subspace generated by the possible values of the label b_2 while keeping the labels b_1 and b_3 fixed.

Written out explicitly, we have

$$B^{b_3}_{b_1tt} = \begin{pmatrix} \left(B^{b_3}_{b_1tt}\right)_{(b_2)_1,(b_2)_1} & \left(B^{b_3}_{b_1tt}\right)_{(b_2)_1,(b_2)_2} & \cdots \\ \left(B^{b_3}_{b_1tt}\right)_{(b_2)_2,(b_2)_1} & \left(B^{b_3}_{b_1tt}\right)_{(b_2)_2,(b_2)_2} & \cdots \\ \vdots & \vdots & \ddots \end{pmatrix} \tag{4.10}$$ {?}

where $(b_2)_j$ denotes the j:th allowed value for the intermediate charge b_2. The allowed values for b_2 depend on b_1 and b_3, in particular we must have that $b_1 \times (b_2)_j = b_3$ is a valid fusion. Note how the number of possible values for b_2 determine the dimension of $B^{b_3}_{b_1tt}$. This also implicitly assumes we have chosen and specific order for our basis.

Here we have expressed $\rho_2(\sigma_1)$ in the full basis of the fusion space $\widetilde{V}_{t^2}$ with basis elements

$$|b_1 b_2 b_3\rangle \equiv \underset{b_1 \quad b_2 \quad b_3}{\overset{t \quad t}{\text{|}\quad\text{|}}} \tag{4.11}$$ {?}

for all possible values of b_1, b_2 and b_3. The action of $\rho_2(\sigma_1)$ on $|b_1(b_2)_j b_3\rangle$ can thus be written as

$$\rho_2(\sigma_1)|b_1(b_2)_j b_3\rangle = \sum_k \left(B^{b_3}_{b_1 tt}\right)_{(b_2)_k,(b_2)_j} |b_1(b_2)_k b_3\rangle. \tag{4.12}$$ {?}

Consider now the larger fusion space $\widetilde{V}_{t^n}$ with standard fusion states

$$|b_1 b_2 \cdots b_n b_{n+1}\rangle \equiv \underset{b_1 \quad b_2 \quad b_3}{\overset{t \quad t}{\text{|}\quad\text{|}}} \cdots \underset{b_{n-1} \quad b_n \quad b_{n+1}}{\overset{t \quad t}{\text{|}\quad\text{|}}}. \tag{4.13}$$ {?}

for all allowed values of the labels $b_1, b_2, \ldots, b_{n+1}$. The braid generator σ_1 still braids the first two t anyons. However, the basis of the space is now larger, giving us a larger representation $\rho_n(\sigma_1)$. The right charge sector for σ_1 can now be seen to consist of all the labels $b_3, b_4, \ldots, b_{n+1}$. The B matrix still only depends on b_1 and b_3, so the block structure is similar to the previous example, but with the exception that there are more possible instances of the b_3 label, due to the presence of $b_4, \ldots b_{n+1}$. Thus,

$$\rho_n(\sigma_1) = \bigoplus_{b_1, b_3, \ldots, b_{n+1}} B^{b_3}_{b_1 tt}. \tag{4.14}$$?eq:rho_n sigma_n repr?

This can also be understood by decomposing the fusion space as

$$\widetilde{V}_{t^n} = \bigoplus_c V^c_{t^2} \otimes \widetilde{V}_{ct^{n-2}} \tag{4.15}$$ {?}

and realizing that $\rho_n(\sigma_1)$ acts only on the $V^c_{t^2}$ part of the space. However, in order to use this decomposition we must first use the F operator to put the state in this fused state.

In order for eq. (4.14) to be valid, and for the blocks to not interweave, i.e. so that we don't have a situation like

$$\rho_n(\sigma_1) = \begin{pmatrix} \left(B^{(b_3)_1}_{(b_1)_1 tt}\right)_{11} & 0 & \left(B^{(b_3)_1}_{(b_1)_1 tt}\right)_{12} & \cdots \\ 0 & \left(B^{(b_3)_1}_{(b_1)_2 tt}\right)_{11} & 0 & \cdots \\ \left(B^{(b_3)_1}_{(b_1)_1 tt}\right)_{21} & 0 & \left(B^{(b_3)_1}_{(b_1)_1 tt}\right)_{22} & \cdots \\ \vdots & \vdots & \vdots & \ddots \end{pmatrix} \tag{4.16}$$ {?}

but rather

$$\rho_n(\sigma_1) = \begin{pmatrix} \left(B^{(b_3)_1}_{(b_1)_1 tt}\right)_{11} & \left(B^{(b_3)_1}_{(b_1)_1 tt}\right)_{12} & 0 & \cdots \\ \left(B^{(b_3)_1}_{(b_1)_1 tt}\right)_{21} & \left(B^{(b_3)_1}_{(b_1)_1 tt}\right)_{22} & 0 & \cdots \\ 0 & 0 & \left(B^{(b_3)_1}_{(b_1)_2 tt}\right)_{11} & \cdots \\ \vdots & \vdots & \vdots & \ddots \end{pmatrix}, \tag{4.17}$$ {?}

we must have that the basis is ordered such that each for each value of b_2 all basis elements for given b_2 follow immediately after each other, and ordered in the same way for each value of b_2. Such a choice for the order of the basis can of course be made, however, this order will most likely cause $\rho_n(\sigma_2), \rho_n(\sigma_3), \ldots, \rho_n(\sigma_{n-1})$ to have charge sectors appearing in non-contiguous order, giving interweaving blocks. To somewhat remedy this, we shall order the basis by the leftmost and rightmost charge sectors b_1 and b_n. The values for these labels can never be mixed, while all other intermediate charges can be mixed. Thus, all representations of the braid generators $\rho_n(\sigma_j)$ respect these outer charge sector blocks. There is however no ordering of the basis that gives a consistent non-interweaving block structure for $\rho_n(\sigma_2)$, see example 5.3.5 as a concrete example of this. It is clear that for each generator σ_j there is a choice of the order of the basis such that its representation $\rho_n(\sigma_j)$ has this described block form. That is, the basis can be partitioned into subsets where each subset spans an invariant subspace under $\rho_n(\sigma_j)$. This discussion is summed up in the following result.

Theorem 4.2.1. *In a given anyon model with non-trivial charge label t, the fusion space $\widetilde{V}_{t^n}$ gives rise to a representation for the braid group B_n, where the generators are represented by*

$$\rho_n(\sigma_j) = P_j^{-1} \left[\bigoplus_{b_1,\ldots,b_j,b_{j+2},\ldots,b_{n+1}} B_{b_j tt}^{b_{j+2}} \right] P_j \tag{4.18}$$ {?}

where P_j is some permutation matrix, permuting the basis of the fusion space as described above.

It is now clear that only the immediate left and right charges b_j and b_{j+2} respectively are essentially all that is needed to determine $\rho_n(\sigma_j)$, regardless of n. Writing out $\rho_n(\sigma_j)$ in the full basis of the fusion space $\widetilde{V}_{t^n}$ gives repeated blocks which may be interweaved as described. The number of times that a given block is repeated is given by the number of corresponding left and right charge sectors in the full basis. More specifically, consider $\rho_n(\sigma_j)$ and the block associated with b_j and b_{j+2}. The number of times this block is repeated is given by the number of possible values for b_j and b_{j+2}, so that the following fusions are allowed

$$\begin{aligned} b_1 \times \cdots \times b_{j-1} &= b_j \\ b_{j+2} \times \cdots \times b_n &= b_{n+1}. \end{aligned} \tag{4.19}$$ {?}

Indeed, the bold symbols in

$$\cdots \underset{b_{j-1}}{\overset{t}{|}} \underset{\boldsymbol{b_j}}{\overset{\boldsymbol{t}}{|}} \underset{\boldsymbol{b_{j+1}}}{\overset{\boldsymbol{t}}{|}} \underset{\boldsymbol{b_{j+2}}}{\overset{t}{|}} \underset{b_{j+3}}{} \cdots \tag{4.20}$$ {?}

are the ones that correspond to one instance of the corresponding block of $\rho_n(\sigma_j)$. For fixed b_j and b_{j+2} there may be several values for the labels $b_1, \ldots, b_{j-1}$ and $b_{j+3}, \ldots, b_{n+1}$ corresponding the same block.

Finally, we verify that the obtained representation indeed satisfies the braid group relations.

Lemma 4.2.2. *The mapping $\rho(\sigma_j) = \bigoplus B_{b_j tt}^{b_{j+2}}$ is a representation of the braid group.*

Proof. It suffices to show that $\rho(\sigma_j)$ satisfies the braid group relations eq. (1.15).

1. The first relation eq. (1.15a) is trivially satisfied since the B operator $B^{b_{j+2}}_{b_j tt}$ holds all labels fixed except b_{j+1}. Thus, for $|j-k| \geq 2$ the free label of $\rho(\sigma_j)$ does not affect $\rho(\sigma_k)$ and vice versa.

2. The second relation eq. (1.15b) requires the hexagon equation. Note that the commutativity forced by the hexagon equation fig. 3.3 implies the braid relation for trivial left charge sector. The case of non-trivial left charge sector is handled by using the F operator to "factor out" the left charge sector, so that $\widetilde{V}_{t^3} = \bigoplus_{b_1,b_4} V^{b_1}_{b_1} \otimes V^{b_4}_{t^3}$ and use the hexagon equation on the $V^{b_4}_{t^3}$-part of the fusion space.

□

4.3 Computing the braid group generators $\rho_n(\sigma_j)$

?⟨sec:general braiding⟩? Consider the fusion space $V^c_{a_1\cdots a_n}$ in a given anyon model, the representation $\rho(\sigma_j)$ gives the anyonic phase introduced to the total wave function when particles a_j and a_j+1 are exchanged (counter)clockwise. Recall from chapter 1 that the braid group is generated by $\sigma_1, \ldots, \sigma_n$, thus it suffices to give expressions for $\rho(\sigma_j)$ in order to be able to compute any braid in a given anyon model.

Before showing how $\rho(\sigma_j)$ is computed, we begin by making our notation slightly more flexible. Consider the fusion space $V^c_{a_1\ldots a_n}$. As we have seen, the fusion states are on the form

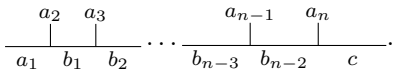

(4.21) {?}

We shall sometimes write such states on the form of the standard basis states of $V^c_{1a_1\ldots a_n}$, i.e. as

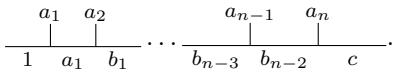

(4.22) {?}

The reason being that it is then simpler to represent braiding of a_1 with a_2. This observation allows us to extend the fusion diagrams with trivial charges when convenient.

In the following results, we use the convention of representing braid operators in the smallest relevant part of the fusion space, as described in section 4.2. Extending the representation to any size of the fusion space involves duplicating blocks depending on the charge sectors of the smaller space.

?⟨res:sigma 1 is R⟩? **Lemma 4.3.1.** *In a general anyon model, in the standard basis of the fusion space $V^c_{a_1\cdots a_n}$ we have*

$$\rho(\sigma_1)_{ij} = \delta_{ij} R^j_{a_1 a_2} \quad \Longleftrightarrow \quad \rho(\sigma_1) = R_{a_1 a_2} \tag{4.23}$$ {?}

in the basis spanned by b_1. The indices i, j range over the possible values for b_1, which essentially represent the basis elements of the reduced space $\langle b_1 \rangle$.

Proof. In the general case, the representation $\rho(\sigma_1)$ for the first generator σ_1 that braids a_1 with a_2, is given by

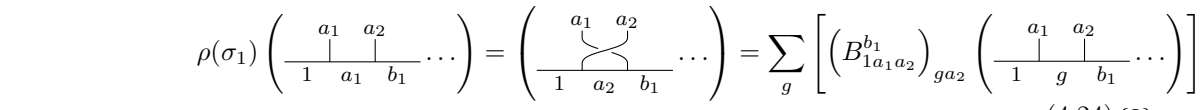

(4.24) {?}

Since 1 fuses trivially we must have $g = a_1$ and thus $\rho(\sigma_1)$ is one-dimensional with

$$\rho(\sigma_1) = \left(B^{b_1}_{1a_1a_2}\right)_{a_1,a_2} = \sum_f \left((F^{-1})^{b_1}_{1a_2a_1}\right)_{fa_2} R^f_{a_1a_2} \left(F^{b_1}_{1a_1a_2}\right)_{a_1f} = R^{b_1}_{a_1a_2}, \tag{4.25}$$

{?}

where the last equality follows from lemma 3.3.1. □

?⟨remark:abuse notation⟩? *Remark* 4.3.1. Above, $\rho(\sigma_1)$ is expressed in the basis for the reduced space $V_{a_1a_2} = \bigoplus_{b_1} V^{b_1}_{a_1a_2}$, having basis determined by the possible anyonic labels b_1. The full space $V^c_{a_1\cdots a_n}$ has basis states $(b_1, \ldots, b_{n-2})$ and we implicitly used the operator on the space reduced to fusion states (b_1).

Extending $\rho(\sigma_1)$ to the full space is straight forward: In order to determine the action of $\rho(\sigma_1)$ on a given fusion state in the basis of the full fusion space it suffices to consider the action of $\rho(\sigma_1)$ on the labels a_1 and a_2 in the given fusion state. This information is precisely captured in the representation of $\rho(\sigma_1)$ in the reduced basis. This results in repeating blocks in the matrix representing $\rho(\sigma_1)$ when considering the basis of the full fusion space. This motivates the slight abuse of notation.

This discussion applies to any braiding operator, and we shall often use this abuse of notation, it should always be clear what part of the space that the operator acts on. See section 4.2 for further discussion of the braid group representation.

?⟨res:sigma j is B⟩? **Lemma 4.3.2.** *In a general anyon model, consider the fusion space $V^c_{a_1\cdots a_n}$ with the standard basis $(b_1, \ldots, b_{n-1})$, then*

$$\rho(\sigma_j) = \bigoplus_{b_{j-2},b_j} B^{b_j}_{b_{j-2}a_ja_{j+1}}, \tag{4.26}$$

{?}

Proof. Note that $\rho(\sigma_j)$ is precisely the B-matrix applied appropriately,

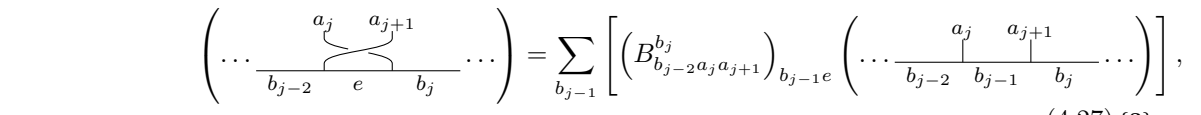

(4.27) {?}

thus the result follows. □

With the convention $b_0 = a_1$ and $b_{-1} = 1$, lemma 4.3.2 subsumes lemma 4.3.1, and also the following result, which we state explicitly for convenience. Recall that $\overline{a}$ denotes the antiparticle of a.

⟨res:sigma n-1 is R⟩ **Lemma 4.3.3.** *In a general anyon model, consider the fusion space $V^1_{a_1\cdots a_n}$ with its standard basis $(b_1, \ldots, b_{n-3})$ (note that $c = 1$ forces $b_{n-2} = \overline{a_n}$), then*

$$\rho(\sigma_{n-1})_{ij} = \delta_{ij} R^{\overline{j}}_{a_{n-1}a_n}, \tag{4.28}$$

{?}

acting on the b_{n-3}-part of the space.

Proof. Since the result of the fusion is assumed to be the trivial particle 1, we must have the indices as follows,

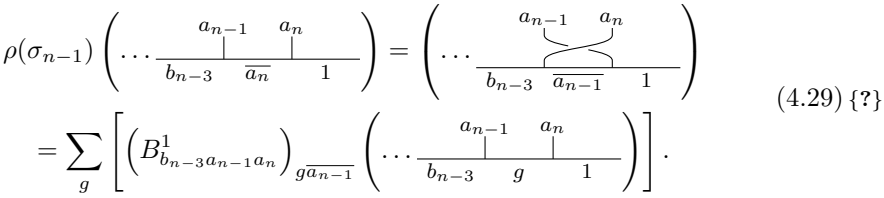

(4.29) {?}

Since the last fusion reads $g \times a_n = 1$ we must have $g = \overline{a_n}$ and thus

$$\begin{aligned}\rho(\sigma_{n-1}) &= \left(B^1_{b_{n-3}a_{n-1}a_n}\right)_{\overline{a_n}a_{n-1}} \\ &= \sum_f \left(\left(F^{-1}\right)^1_{b_{n-3}a_n a_{n-1}}\right)_{f\overline{a_{n-1}}} R^f_{a_{n-1}a_n} \left(F^1_{b_{n-3}a_{n-1}a_n}\right)_{\overline{a_n}f} \\ &= R^{\overline{b_{n-3}}}_{a_{n-1}a_n}\end{aligned} \tag{4.30}$$ {?}

where the last equality follows from lemma 3.3.1. □

Remark 4.3.2. Note that $\rho(\sigma_1)$ and $\rho(\sigma_{n-1})$ are equal in the restricted basis, up to charge conjugation of the basis. Furthermore, note that if time is reversed, the roles of $\rho(\sigma_1)$ and $\rho(\sigma_j)$ are interchanged. Reversing the fusion in time means reading the fusion diagram from right/bottom to left/top. This is an example of time reversal symmetry; time reversal corresponds to charge conjugation, see [20].

Time reversal as charge conjugation is also simply manifested in the following lemma, as a result of lemma 4.3.1 and 4.3.3.

Lemma 4.3.4. *In the standard basis the R matrix can be written as*

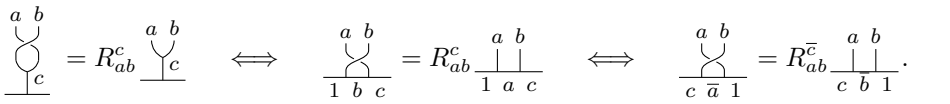

(4.31) {?}

4.4 Anyonic exchange operator U_p

?⟨sec:general Up⟩? Given any abstract anyon model, single out a non-trivial anyonic charge t and consider exchange of a pair of anyons around p enclosed anyons. That is consider the fusion space $\widetilde{V}_{t^{p+2}}$.

In the standard basis of $\widetilde{V}_{t^n}$, we can compute the braid group generators $\rho_n(\sigma_j)$ for $j = 1, 2, \ldots, n-1$ as shown in section 4.3. The exchange operator U_p (as introduced in section 1.2) is then

$$U_p = \sigma_1\sigma_2\cdots\sigma_p\sigma_{p+1}\sigma_p\cdots\sigma_2\sigma_1, \tag{4.32}$$ {?}

c.f. **??**. However, working in the standard basis is rather problematic for computing U_p, instead we change basis.

With the F matrix we change basis from the standard basis to a basis where the enclosed p anyons are fused. If $p = 2$ we have

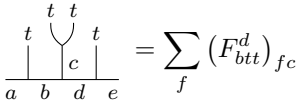

$$= \sum_f \left(F^d_{btt}\right)_{fc}$$

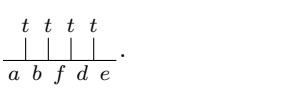

. (4.33) {?}

This extends to arbitrary number p of enclosed particles by repeated application of the F matrix. For any $p \geq 2$ we can thus change basis from the standard basis to the fused basis

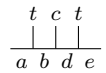

(4.34) {?}

where c is the resulting charge of the fused enclosed p particles. More explicitly that is

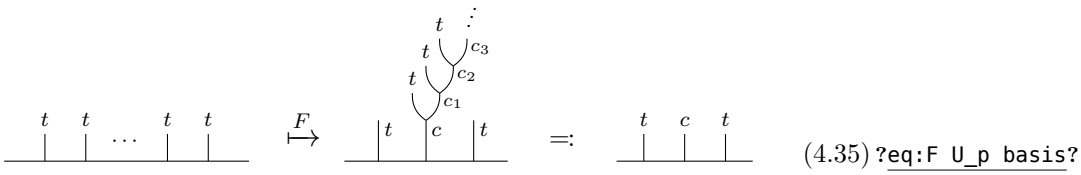

(4.35) ?eq:F U_p basis?

The intermediate charge c depends on p such that c is a possible result of the fusion $\underbrace{t \times t \times \cdots \times t}_{p}$. Explicitly that is

$$\begin{aligned}
&p = 0 \implies c = 1 \\
&p = 1 \implies c = t \\
&p = 2 \implies c \text{ is a possible result of the fusion } t \times t \\
&p = 3 \implies c \text{ is a possible result of the fusion } t \times t \times t \\
&\quad \vdots
\end{aligned} \tag{4.36} \{?\}$$

This can be written as a decomposition of the fusion space

$$\widetilde{V}_{t^{p+2}} = \bigoplus_c V^c_{t^p} \otimes \widetilde{V}_{tct}. \tag{4.37} \{?\}$$

The braid U_p acts only on the subspace $\widetilde{V}_{tct}$. In particular, the braid corresponding to U_p does not depend on the intermediate charges $c_1, c_2, \ldots, c_{p-2}$.

We are now ready to compute U_p for general p,

U_p 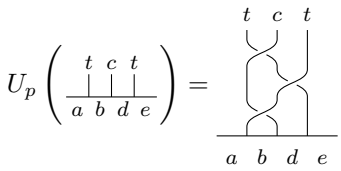

$$= \sum_f \left(B^d_{act}\right)_{fb}$$ 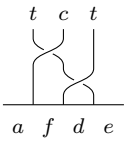

(4.38) ?eq:U_p braid?

$$= \sum_f \left(B^d_{act}\right)_{fb} \sum_g \left(B^e_{ftt}\right)_{gd}$$ 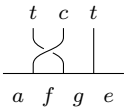

$$= \sum_f \left(B^d_{act}\right)_{fb} \sum_g \left(B^e_{ftt}\right)_{gd} \sum_h \left(B^g_{atc}\right)_{hf}$$ 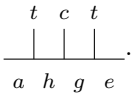

.

Thus, we have the following theorem.

?⟨thm:general Up⟩? **Theorem 4.4.1.** *In a given abstract anyon model, exchange of a pair of t-anyons around p enclosed t-anyons is described by the exchange operator U_p given by*

$$U_p = \bigoplus_c U_{1,c} \tag{4.39}$$ {?}

where $U_{1,c}$ denotes the exchange operator for two t anyons around one anyon of type c, and c ranges over all possible total charges of the p enclosed anyons, that is, the possible total charges c for the fusion space $V^c_{t^p}$. $U_{1,c}$ is given by

$U_{1,c}$ 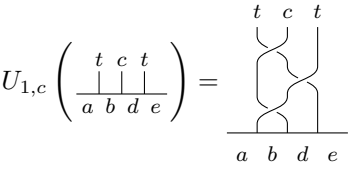

$$= \sum_{f,g,h} \left(B^d_{act}\right)_{fb} \left(B^e_{ftt}\right)_{gd} \left(B^g_{atc}\right)_{hf}$$ 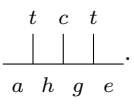

.

(4.40) {?}

4.5 Abelian representations: Abelian anyons

In this section we show how Abelian anyons are modeled in the framework of abstract anyon models. First, note that Abelian anyons are characterized by that each fusion has a unique result, i.e. fusion of a with b results in a unique label c for all a and b,

$$a \times b = c. \tag{4.41}$$ {?}

As a consequence of this we have that any fusion space of Abelian anyons is trivial and one-dimensional. All intermediate charges are uniquely determined by the simple fusion rules.

As a first example we shall see how fermionic statistics fits into the framework of abstract anyon models. In the computations, recall that $R^c_{ab} = R^c_{ba}$. In this section we deviate from our convention and denote the trivial particle by 0 and positive integers denote non-trivial label, the reason being that fusion is defined as the sum of the labels.

Example 4.5.1 ($\mathbb{Z}_2^{(n)}$)**.** Let the set of anyonic charges be $\mathbb{Z}_2 = \{0, 1\}$, the trivial vacuum particle 0 and one non-trivial particle 1, with corresponding fusion corresponding to addition in $\mathbb{Z}_2$, in particular

$$1 \times 1 = 0. \tag{4.42}$$ {?}

Since the fusion spaces are trivial, we take $F^{a+b+c}_{abc} = 1$ for all a, b and c. Thus, the pentagon equation eq. (3.34) is trivial and the hexagon equation eq. (3.35) reduces to

$$\begin{aligned} & R^g_{ac} \left(F^d_{bac}\right)^g_e R^e_{ab} = \sum_f \left(F^d_{bca}\right)^g_f R^d_{af} \left(F^d_{abc}\right)^f_e \\ \iff\ & R^{a+c}_{ac} R^{a+b}_{ab} = \sum_f R^{a+b+c}_{af}. \end{aligned} \tag{4.43}$$ {?}

We have $d = a + b + c$ from the F symbol $\left(F^d_{bac}\right)$, this gives $a + f = a + b + c$, i.e. $f = b + c$. The hexagon equation is thus reduced to

$$R^{a+c}_{ac} R^{a+b}_{ab} = R^{a+b+c}_{a,(b+c)}. \tag{4.44}$$ {?}

Since $R^{a+b}_{ab} = 1$ if a or b equals 0. The only non-trivial case is

$$R^0_{11} R^0_{11} = 1 \quad \iff \quad R^0_{11} = \pm 1. \tag{4.45}$$ {?}

Thus, the chosen model, i.e. charges and fusion modeled by $\mathbb{Z}_2$ gives two distinct Abelian anyon models which we parametrize by $n = 0, 1$ so that we have

$$R^0_{11} = e^{in\pi}. \tag{4.46}$$ {?}

We denote these two models by $\mathbb{Z}_2^{(n)}$ for $n = 0, 1$. In conclusion, we see that fermionic statistics are modeled by $\mathbb{Z}_2^{(1)}$. Similarly, bosonic statistics is modeled by $\mathbb{Z}_2^{(0)}$.

In the above example we considered fusion modeled by $\mathbb{Z}_2$ and saw that this gives rise to two distinct models. Before stating the general result, we first extend the example to see more clearly how the hexagon equation determines the R matrices.

Example 4.5.2 ($\mathbb{Z}_3^{(n)}$)**.** Let fusion be modeled on $\mathbb{Z}_3$, so that the the charge label set is $\mathbb{Z}_3 = \{0, 1, 2\}$ and fusion is given by addition modulo 3,

$$a \times b = [a + b]_3. \tag{4.47}$$ {?}

The only non-trivial instances of the hexagon equation are

$$\begin{aligned} \left(R^2_{11}\right)^2 &= R^0_{12} \\ \left(R^2_{12}\right)^2 &= R^2_{11} \\ \left(R^1_{22}\right)^2 &= R^2_{12} \\ R^2_{11} R^0_{12} &= 1 \\ R^0_{12} R^1_{22} &= 1. \end{aligned} \tag{4.48}$$ {?}

The first two equations combined give $\left(R^2_{11}\right)^3 = 1 \iff R^2_{11} = e^{i2\pi n/3}$. Each of the three solutions for R^2_{11}, corresponding to $n = 0, 1, 2$ give a solution for R^2_{12} and R^1_{22}. This gives rise to three distinct models:

- $\mathbb{Z}_3^{(0)}$: The trivial solution $R^{a+b}_{ab} \equiv 1$ for all a, b.
- $\mathbb{Z}_3^{(1)}$: Take $R^2_{11} = e^{i2\pi/3}$, the fourth equation gives $R^0_{12} = e^{i4\pi/3}$ and the fifth equation gives $R^1_{22} = e^{i2\pi/3}$.
- $\mathbb{Z}_3^{(2)}$: Take $R^2_{11} = e^{i4\pi/3}$, the fourth equation gives $R^0_{12} = e^{i2\pi/3}$ and the fifth equation gives $R^1_{22} = e^{i2\pi/3}$.

The possible solutions can be compactly written as

$$R^{a+b}_{ab} = e^{i\frac{2\pi n}{3}ab} \tag{4.49}$$ {?}

Indeed, the more general result holds, discussed further in [13], motivating the following definition.

Definition 4.5.1. The Abelian model $\mathbb{Z}_N^{(n)}$ is given by taking the charge label set to be $\mathbb{Z}_N$ and fusion given by addition modulo N,

$$a \times b = [a + b]_N. \tag{4.50}$$ {?}

In this model we have

$$F^{a+b+c}_{abc} \equiv 1 \tag{4.51}$$?eq:abelian F?

$$R^{a+b}_{ab} = e^{i\frac{2\pi n}{N}ab}. \tag{4.52}$$?eq:abelian R?

By definition 3.5.1 we thus have

$$B^{a+b+c}_{abc} = R^{b+c}_{bc}, \tag{4.53}$$?eq:abelian B?

note that the left charge a does not enter the expression.

Consider $\mathbb{Z}_N^{(n)}$ and the fusion space $\widetilde{V}_{1^m}$ which now is one-dimensional containing one standard fusion state

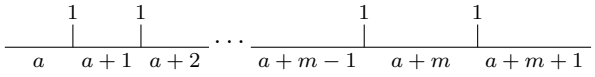

(4.54) {?}

where a is any charge in $\mathbb{Z}_N$ representing the fact that the m considered anyons may be part of a larger set of anyons. In lemma 4.3.2 we showed

$$\rho(\sigma_j) = B^{b_j}_{b_{j-2}a_j a_{j+1}}. \tag{4.55}$$ {?}

Equations (4.52) and (4.53) reduces this to

$$\rho(\sigma_j) = R^2_{11} = e^{i\frac{2\pi n}{N}} \tag{4.56}$$ {?}

for all j. This precisely models Abelian anyons with anyonic phase $\alpha = \frac{2n}{N}$, i.e. any fractional phase. What we have obtained here precisely corresponds to the

discussion of Abelian anyons in **??** which was treated before we had the general framework of abstract anyon models.

Furthermore, in the fusion space $\widetilde{V}_{1^m}$ of the $\mathbb{Z}_N^{(n)}$ model, the exchange operator U_p is

$$\begin{aligned} U_p &= \rho(\sigma_1)\rho(\sigma_2)\cdots\rho(\sigma_p)\rho(\sigma_{p+1})\rho(\sigma_p)\cdots\rho(\sigma_2)\rho(\sigma_1) \\ &= (\rho(\sigma_1))^{2p+1} = e^{i(2p+1)\alpha}. \end{aligned} \tag{4.57}$$ {?}

Theorem 4.4.1 is clearly not needed in the Abelian case, we instantly have all information of U_p. However, theorem 4.4.1 still applies, first change basis to the fused basis

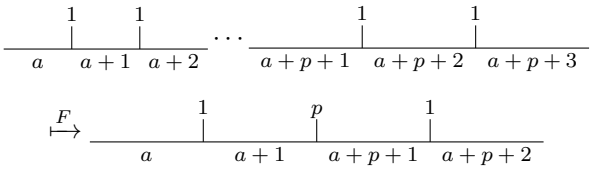

and theorem 4.4.1 gives

$$U_p\left(\begin{array}{c}1\ c\ 1\\ |\ |\ |\\ \hline a\ b\ d\ e\end{array}\right) = \sum_f \left(B^d_{act}\right)_{fb} \sum_g \left(B^e_{ftt}\right)_{gd} \sum_h \left(B^g_{atc}\right)_{hf} \begin{array}{c}1\ c\ 1\\ |\ |\ |\\ \hline a\ h\ g\ e\end{array}. \tag{4.58}$$ {?}

As we've seen, the intermediate charges play no role, indeed the fusion space is one dimensional. In the $\mathbb{Z}_N^{(n)}$model this expression for U_p immediately reduces to

$$U_p = R_{c1}R_{11}R_{1c} = e^{ip\alpha\pi}e^{i\alpha\pi}e^{ip\alpha\pi} = e^{i(2p+1)\alpha\pi} \tag{4.59}$$ {?}

as expected.

Chapter 5

Fibonacci anyons

?⟨fibonacci anyons⟩? The Fibonacci anyon model is one of the simplest non-Abelian anyon models containing all the interesting features of non-Abelian anyons. It is commonly studied as a prototypical example of non-Abelian anyons. Another common model is the Ising model, however Ising anyons cannot be used for general quantum computation.

Fibonacci anyons can be realized in the $k = 3$ Reed-Rezayi state [21], cf. section 1.4. In this state there will be additional Abelian phases present, which do not occur in the model that we shall describe in this chapter. These additional Abelian phases may have physical consequences for some experiments, but they are not of interest for the higher-dimensional non-Abelian representation, which is what we are primarily interested in. In the context of conformal field theory the Fibonacci model is called the Yang-Lee model.

This chapter is partly based on [12, 21, 14]. The literature is rather vague on deriving the properties of Fibonacci anyons, in this chapter we spelled out the details more clearly.

5.1 Preliminaries

:fibonacci preliminaries⟩? The Fibonacci anyon model consists of two particle types, 1 (the mandatory trivial particle type) and τ (non-trivial) with the corresponding fusion rules

$$1 \times 1 = 1, \quad 1 \times \tau = \tau \times 1 = \tau, \quad \tau \times \tau = 1 + \tau. \tag{5.1}$$ {?}

Furthermore, τ is its own anti-particle $\overline{\tau}$. We shall refer to the τ anyon as Fibonacci anyons.

As we shall now see, the dimension of the fusion space of n Fibonacci anyons grows as the Fibonacci numbers as n increases. Thus motivating the name of the model. Consider the fusion spaces $V_{\tau^n}^1$, where τ^n denotes n repetitions of τ. This is the space of possible fusions of n Fibonacci anyons, having total charge

1. Writing out the canonical basis for these spaces we find

$$
\begin{aligned}
V^1_{\tau^2} &: \left\{ \begin{array}{c} \tau\ \tau \\ \vert\ \vert \\ \hline 1\ \tau\ 1 \end{array} \right\} \\
V^1_{\tau^3} &: \left\{ \begin{array}{c} \tau\ \tau\ \tau \\ \vert\ \vert\ \vert \\ \hline 1\ \tau\ \tau\ 1 \end{array} \right\} \\
V^1_{\tau^4} &: \left\{ \begin{array}{c} \tau\ \tau\ \tau\ \tau \\ \vert\ \vert\ \vert\ \vert \\ \hline 1\ \tau\ \mathbf{1}\ \tau\ 1 \end{array}, \begin{array}{c} \tau\ \tau\ \tau\ \tau \\ \vert\ \vert\ \vert\ \vert \\ \hline 1\ \tau\ \boldsymbol{\tau}\ \tau\ 1 \end{array} \right\} \\
V^1_{\tau^5} \simeq \widetilde{V}_\tau &: \left\{ \begin{array}{c} \tau\ \tau\ \tau\ \tau\ \tau \\ \vert\ \vert\ \vert\ \vert\ \vert \\ \hline 1\ \tau\ \mathbf{1}\ \boldsymbol{\tau}\ \tau\ 1 \end{array}, \begin{array}{c} \tau\ \tau\ \tau\ \tau\ \tau \\ \vert\ \vert\ \vert\ \vert\ \vert \\ \hline 1\ \tau\ \boldsymbol{\tau}\ \mathbf{1}\ \tau\ 1 \end{array}, \begin{array}{c} \tau\ \tau\ \tau\ \tau\ \tau \\ \vert\ \vert\ \vert\ \vert\ \vert \\ \hline 1\ \tau\ \boldsymbol{\tau}\ \boldsymbol{\tau}\ \tau\ 1 \end{array} \right\} \\
&\simeq \left\{ \begin{array}{c} \tau \\ \vert \\ \hline 1\ \tau \end{array}, \begin{array}{c} \tau \\ \vert \\ \hline \tau\ 1 \end{array}, \begin{array}{c} \tau \\ \vert \\ \hline \tau\ \tau \end{array} \right\} \\
V^1_{\tau^6} \simeq \widetilde{V}_{\tau^2} &: \left\{ \begin{array}{c} \tau\ \tau\ \tau\ \tau\ \tau\ \tau \\ \vert\ \vert\ \vert\ \vert\ \vert\ \vert \\ \hline 1\ \tau\ \mathbf{1}\ \boldsymbol{\tau}\ \mathbf{1}\ \tau\ 1 \end{array}, \begin{array}{c} \tau\ \tau\ \tau\ \tau\ \tau\ \tau \\ \vert\ \vert\ \vert\ \vert\ \vert\ \vert \\ \hline 1\ \tau\ \mathbf{1}\ \boldsymbol{\tau}\ \boldsymbol{\tau}\ \tau\ 1 \end{array}, \right. \\
&\qquad \left. \begin{array}{c} \tau\ \tau\ \tau\ \tau\ \tau\ \tau \\ \vert\ \vert\ \vert\ \vert\ \vert\ \vert \\ \hline 1\ \tau\ \boldsymbol{\tau}\ \boldsymbol{\tau}\ \mathbf{1}\ \tau\ 1 \end{array}, \begin{array}{c} \tau\ \tau\ \tau\ \tau\ \tau\ \tau \\ \vert\ \vert\ \vert\ \vert\ \vert\ \vert \\ \hline 1\ \tau\ \boldsymbol{\tau}\ \mathbf{1}\ \boldsymbol{\tau}\ \tau\ 1 \end{array}, \begin{array}{c} \tau\ \tau\ \tau\ \tau\ \tau\ \tau \\ \vert\ \vert\ \vert\ \vert\ \vert\ \vert \\ \hline 1\ \tau\ \boldsymbol{\tau}\ \boldsymbol{\tau}\ \boldsymbol{\tau}\ \tau\ 1 \end{array} \right\} \\
&\simeq \left\{ \begin{array}{c} \tau\ \tau \\ \vert\ \vert \\ \hline 1\ \tau\ 1 \end{array}, \begin{array}{c} \tau\ \tau \\ \vert\ \vert \\ \hline 1\ \tau\ \tau \end{array}, \begin{array}{c} \tau\ \tau \\ \vert\ \vert \\ \hline \tau\ \tau\ 1 \end{array}, \begin{array}{c} \tau\ \tau \\ \vert\ \vert \\ \hline \tau\ 1\ \tau \end{array}, \begin{array}{c} \tau\ \tau \\ \vert\ \vert \\ \hline \tau\ \tau\ \tau \end{array} \right\}.
\end{aligned}
\tag{5.2}
$$

Note that $V^1_{\tau^n} \simeq \widetilde{V}_{\tau^{n-4}}$ in the sense that the two τ anyons on the left and right side in $V^1_{\tau^n}$ give all possible charge sectors for $\widetilde{V}_{\tau^{n-4}}$. Continuing this list is straight forward. Note that the bottom line in the fusion diagrams of the fusion states in the bases can be seen as strings of τ and 1, having 1τ at the start and $\tau 1$ at the end. Furthermore, the string is subject to the condition that 1 may not be followed by 1. Indeed, 1 on the bottom row fuses with τ from the top, to give τ. We now make this more precise.

?⟨def:fibonacci strings⟩? **Definition 5.1.1.** A Fibonacci string of length n on two symbols, say 1 and τ, is a string of length n on the symbols 1 and τ subject to the condition that 1 may not be followed by 1.

There are two Fibonacci string of length one, namely 1 and τ, of length two we have three Fibonacci strings, $1\tau, \tau 1, \tau\tau$, etc. Note that the free charge labels, marked in bold in the above fusion states, are precisely Fibonacci strings. Let f_n denote the number of Fibonacci strings of length n. We then have

$$
\begin{aligned}
&\dim V_{\tau^n} = \dim V^1_{\tau^n} + \dim V^\tau_{\tau^n} = f_{n-3} + f_{n-2} = f_{n-1} \\
&\dim \widetilde{V}_{\tau^n} = f_{n+1}.
\end{aligned}
\tag{5.3}
$$

The following result determines the number f_n.

:fibonacci string length⟩? **Lemma 5.1.1.** *The number f_n of Fibonacci strings of length n is* $\mathrm{Fib}(n+2)$*, where* $\mathrm{Fib}(n)$ *denotes the n:th Fibonacci number given by*

$$
\begin{aligned}
\mathrm{Fib}(0) &= 0 \\
\mathrm{Fib}(1) &= 1 \\
\mathrm{Fib}(n+1) &= \mathrm{Fib}(n) + \mathrm{Fib}(n-1).
\end{aligned}
\tag{5.4}
$$

Proof. Let f_n denote the number of Fibonacci strings of length n, and let f_n^a denote the number of Fibonacci strings of length n ending with a, where $a = 1, \tau$. We then have $f_n = f_n^1 + f_n^\tau$. This, together with the definition of Fibonacci strings gives

$$\begin{aligned} f_{n+1} &= f_{n+1}^1 + f_{n+1}^\tau \\ &= f_n^\tau + \left(f_n^1 + f_n^\tau\right) \\ &= \left(f_n^\tau + f_n^1\right) + \left(f_{n-1}^1 + f_{n-1}^\tau\right) \\ &= f_n + f_{n-1}. \end{aligned} \tag{5.5}$$ {?}

This is precisely the recursion relation for the Fibonacci numbers. Finally, initial values $f_1 = 2, f_2 = 3$ shows that

$$f_n = \mathrm{Fib}(n+2). \tag{5.6}$$ {?}

□

We can now use this to characterize the dimension of fusion spaces.

i fusion space dimension⟩?

Lemma 5.1.2. *The dimension of the fusion space with n Fibonacci, with different charge sectors, is given by*

$$\begin{aligned} \dim V_{\tau^n}^1 &= \mathrm{Fib}(n-1) \\ \dim V_{\tau^n}^\tau &= \mathrm{Fib}(n) \\ \dim V_{\tau^n} &= \mathrm{Fib}(n+1) \\ \dim \widetilde{V}_{\tau^n} &= \mathrm{Fib}(n+3) \end{aligned} \tag{5.7}$$ {?}

Proof. The first equality follows from

$$\dim V_{\tau^n}^1 = f_{n-3} = \mathrm{Fib}((n-3)+2) = \mathrm{Fib}(n-1). \tag{5.8}$$ {?}

Next,

$$\dim V_{\tau^n}^\tau = \dim V_{\tau^{n+1}}^1 = \mathrm{Fib}(n). \tag{5.9}$$ {?}

Finally,

$$\dim \widetilde{V}_{\tau^n} = f_{n+1} = \mathrm{Fib}((n+1)+2) = \mathrm{Fib}(n+3). \tag{5.10}$$ {?}

□

The above approach, using Fibonacci strings, reveals how the possible intermediate charges determine how the Fibonacci fusion space grows. A more direct approach is to identify the labels 1 and τ by the vectors

$$1 \equiv \begin{pmatrix} 1 \\ 0 \end{pmatrix}, \quad \tau \equiv \begin{pmatrix} 0 \\ 1 \end{pmatrix}. \tag{5.11}$$ {?}

We can then represent fusion with τ by the matrix

$$\begin{pmatrix} 0 & 1 \\ 1 & 1 \end{pmatrix} \tag{5.12}$$ {?}

so that

$$\begin{aligned} \tau \times 1 &= \begin{pmatrix} 0 & 1 \\ 1 & 1 \end{pmatrix} \begin{pmatrix} 1 \\ 0 \end{pmatrix} = \begin{pmatrix} 0 \\ 1 \end{pmatrix} = \tau \\ \tau \times \tau &= \begin{pmatrix} 0 & 1 \\ 1 & 1 \end{pmatrix} \begin{pmatrix} 0 \\ 1 \end{pmatrix} = \begin{pmatrix} 1 \\ 1 \end{pmatrix} = 1 + \tau. \end{aligned} \tag{5.13}$$ {?}

We can now use this to determine fusion of n Fibonacci anyons,

$$\begin{pmatrix} 0 & 1 \\ 1 & 1 \end{pmatrix}^n \begin{pmatrix} 1 \\ 0 \end{pmatrix} = \begin{pmatrix} \mathrm{Fib}(n-1) \\ \mathrm{Fib}(n) \end{pmatrix} = \mathrm{Fib}(n-1)1 + \mathrm{Fib}(n)\tau. \tag{5.14}$$ {?}

This counts the dimension of the fusion spaces $V^1_{\tau^n}$ and $V^\tau_{\tau^n}$, respectively, in a agreement with lemma 5.1.2.

As we have seen in chapter 3, an anyon model is determined by the corresponding F- and R-matrices. We continue determining these operators for the case of Fibonacci anyons.

5.2 Determining the model: Computing the F and R matrices

TODO: Write down computation.

TODO: Discuss the free parameter in F that is fixed by gauge fixing. Preskill p. 60.

$$\begin{aligned} R_{\tau\tau} &= \begin{pmatrix} R^1_{\tau\tau} & 0 \\ 0 & R^\tau_{\tau\tau} \end{pmatrix} = \begin{pmatrix} e^{4\pi i/5} & 0 \\ 0 & e^{-3\pi i/5} \end{pmatrix}, \\ F_{\tau\tau\tau} &= \begin{pmatrix} F^{11}_{\tau\tau\tau} & F^{1\tau}_{\tau\tau\tau} \\ F^{\tau 1}_{\tau\tau\tau} & F^{\tau\tau}_{\tau\tau\tau} \end{pmatrix} = \begin{pmatrix} \varphi^{-1} & \varphi^{-1/2} \\ \varphi^{-1/2} & -\varphi^{-1} \end{pmatrix}. \end{aligned} \tag{5.15}$$ {?}

For convenience, when discussing Fibonacci anyons, let

$$F \coloneqq F^\tau_{\tau\tau\tau}, \quad R \coloneqq R_{\tau\tau}, \quad B \coloneqq F^{-1}RF. \tag{5.16}$$ {?}

5.3 Braiding of Fibonacci anyons

In this section we shall compute the braid group generators for various number of Fibonacci anyons. Ultimately, we shall compute $\rho(\sigma_j)$ for $V^1_{\tau^n}$. Having trivial total charge represents the fact that we have exactly n Fibonacci anyons. If the total charge would be τ, there would really be $n+1$ Fibonacci anyons available. As we shall see, there will be some subtleties regarding different charge sectors, i.e. different total charge, when considering braiding of intermediate τ anyons in $V^1_{\tau^n}$. We begin with some elementary examples.

Recall the decomposition

$$V_{a_1\cdots a_n} = \bigoplus_c V^c_{a_1\cdots a_n}, \tag{5.17}$$ {?}

in particular

$$V_{\tau^n} = V^1_{\tau^n} \oplus V^\tau_{\tau^n}. \tag{5.18}$$ {?}

5.3.1 Prototypical examples

Example 5.3.1 (Braiding in V_{τ^2})**.** The two charge sectors of V_{τ^2} have the standard basis

$$V^1_{\tau\tau} = \mathrm{span}\left\{ \begin{array}{c} \tau\ \tau \\ \hline 1\ \tau\ \mathbf{1} \end{array} \right\}, \quad V^\tau_{\tau\tau} = \mathrm{span}\left\{ \begin{array}{c} \tau\ \tau \\ \hline 1\ \tau\ \boldsymbol{\tau} \end{array} \right\}. \tag{5.19}$$ {?}

That is, the fusion space V_{τ^2} is two-dimensional and we denote the ordered basis by $\{1, \tau\}$. Since there is only two τ-anyons, there are only one generator for the braid group, σ_1. We compute $\rho(\sigma_1)$ by considering its action on the standard fusion states,

$$\begin{aligned}\rho(\sigma_1)\,&\underset{1\ \tau\ 1}{\overset{\tau\ \tau}{|\ |\ |}} = \underset{1\ \tau\ 1}{\overset{\tau\ \tau}{\smile\!\frown}} = R^1_{\tau\tau}\,\underset{1\ \tau\ 1}{\overset{\tau\ \tau}{|\ |\ |}} \\ \rho(\sigma_1)\,&\underset{1\ \tau\ \tau}{\overset{\tau\ \tau}{|\ |\ |}} = \underset{1\ \tau\ \tau}{\overset{\tau\ \tau}{\smile\!\frown}} = R^\tau_{\tau\tau}\,\underset{1\ \tau\ \tau}{\overset{\tau\ \tau}{|\ |\ |}}.\end{aligned} \tag{5.20}$$

Thus we have

$$\left.\begin{aligned}\rho(\sigma_1)_{11} &= R^1_{\tau\tau} \\ \rho(\sigma_1)_{1\tau} &= 0 \\ \rho(\sigma_1)_{\tau\tau} &= R^\tau_{\tau\tau} \\ \rho(\sigma_1)_{\tau 1} &= 0\end{aligned}\right\} \quad\Longleftrightarrow\quad \rho(\sigma_1) = \begin{pmatrix} R^1_{\tau\tau} & 0 \\ 0 & R^\tau_{\tau\tau}\end{pmatrix}. \tag{5.21}$$

This also follows immediately from lemma 4.3.1.

Example 5.3.2 (Braiding in V_{τ^3})**.** The two charge sectors of V_{τ^3} have the standard basis

$$V^1_{\tau\tau\tau} = \operatorname{span}\left\{\underset{1\ \tau\ \boldsymbol{\tau}\ \mathbf{1}}{\overset{\tau\ \tau\ \tau}{|\ |\ |\ |}}\right\}, \quad V^\tau_{\tau\tau\tau} = \operatorname{span}\left\{\underset{1\ \tau\ \mathbf{1}\ \boldsymbol{\tau}}{\overset{\tau\ \tau\ \tau}{|\ |\ |\ |}}, \underset{1\ \tau\ \boldsymbol{\tau}\ \boldsymbol{\tau}}{\overset{\tau\ \tau\ \tau}{|\ |\ |\ |}}\right\}. \tag{5.22}$$

That is, the fusion space V_{τ^3} is three-dimensional, and we denote the ordered basis by $\{\tau 1, 1\tau, \tau\tau\}$. Since there are three τ-anyons, there are two generators for the braid group, σ_1 and σ_2. Lemma 4.3.1 gives

$$\begin{aligned}\rho(\sigma_1)_{(\tau 1),(\tau 1)} &= R^\tau_{\tau\tau} \\ \rho(\sigma_1)_{(1\tau),(1\tau)} &= R^1_{\tau\tau} \\ \rho(\sigma_1)_{(\tau\tau),(\tau\tau)} &= R^\tau_{\tau\tau} \\ \rho(\sigma_1)_{i,j} &= 0 \text{ for } i \neq j.\end{aligned} \tag{5.23}$$

In matrix form that is

$$\rho(\sigma_1) = \begin{pmatrix} R^\tau_{\tau\tau} & & \\ & R^1_{\tau\tau} & \\ & & R^\tau_{\tau\tau}\end{pmatrix} = R^\tau_{\tau\tau} \oplus R. \tag{5.24}$$

The empty entries in the matrix are zero, we shall use this convention throughout the thesis, to make the notation less cluttered.

Lemma 4.3.3 gives

$$\rho(\sigma_2)_{(\tau 1),(\tau 1)} = R^\tau_{\tau\tau}. \tag{5.25}$$

We compute $\rho(\sigma_2)$ for the τ-charge sector by considering its action on the standard fusion states

$$\begin{aligned}\rho(\sigma_2)\,&\underset{1\ \tau\ \mathbf{1}\ \tau}{\overset{\tau\ \tau\ \tau}{|\ |\ |\ |}} = \underset{1\ \tau\ \mathbf{1}\ \tau}{\overset{\tau\ \tau\ \tau}{|\ \smile\!\frown}} = (B^\tau_{\tau\tau\tau})_{11}\,\underset{1\ \tau\ \mathbf{1}\ \tau}{\overset{\tau\ \tau\ \tau}{|\ |\ |\ |}} + (B^\tau_{\tau\tau\tau})_{\tau 1}\,\underset{1\ \tau\ \boldsymbol{\tau}\ \tau}{\overset{\tau\ \tau\ \tau}{|\ |\ |\ |}}, \\ \rho(\sigma_2)\,&\underset{1\ \tau\ \boldsymbol{\tau}\ \tau}{\overset{\tau\ \tau\ \tau}{|\ |\ |\ |}} = \underset{1\ \tau\ \boldsymbol{\tau}\ \tau}{\overset{\tau\ \tau\ \tau}{|\ \smile\!\frown}} = (B^\tau_{\tau\tau\tau})_{1\tau}\,\underset{1\ \tau\ \mathbf{1}\ \tau}{\overset{\tau\ \tau\ \tau}{|\ |\ |\ |}} + (B^\tau_{\tau\tau\tau})_{\tau\tau}\,\underset{1\ \tau\ \boldsymbol{\tau}\ \tau}{\overset{\tau\ \tau\ \tau}{|\ |\ |\ |}}.\end{aligned} \tag{5.26}$$

Thus we have

$$\begin{aligned}\rho(\sigma_2)_{(1\tau),(1\tau)} &= (B^\tau_{\tau\tau\tau})_{11}\\ \rho(\sigma_2)_{(1\tau),(\tau\tau)} &= (B^\tau_{\tau\tau\tau})_{1\tau}\\ \rho(\sigma_2)_{(\tau\tau),(1\tau)} &= (B^\tau_{\tau\tau\tau})_{\tau 1}\\ \rho(\sigma_2)_{(\tau\tau),(\tau\tau)} &= (B^\tau_{\tau\tau\tau})_{\tau\tau}\,.\end{aligned} \tag{5.27}$$ {?}

In matrix form that is

$$\rho(\sigma_2) = \begin{pmatrix} R^\tau_{\tau\tau} & & \\ & B_{11} & B_{1\tau} \\ & B_{\tau 1} & B_{\tau\tau} \end{pmatrix} = R^\tau_{\tau\tau} \oplus B. \tag{5.28}$$ {?}

Example 5.3.3 (Braiding in $V^1_{\tau^4}$)**.** Consider $V^1_{\tau^4}$, this is the smallest non-trivial proper fusion space having dimension two. The fusion space is proper in the sense that the there is only one charge sector and it is the trivial (vacuum) charge sector. That is, there are really only 4 Fibonacci anyons. The following result determines the braid group representation determined by exchange of Fibonacci anyons in the standard basis of $V^1_{\tau^4}$. This shall be used in the discussion of topological quantum computation with Fibonacci anyons in section 6.2.

fibonacci qubit braiding⟩?

Proposition 5.3.1. *The representation of the braid group generators determined by $V^1_{\tau^4}$ in the standard basis is*

$$\rho(\sigma_1) = R, \quad \rho(\sigma_2) = B, \quad \rho(\sigma_3) = R. \tag{5.29}$$ {?}

Proof. Lemma 4.3.1 gives

$$\rho(\sigma_1) = B^\tau_{1\tau\tau} = R_{\tau\tau} = \begin{pmatrix} R^1_{\tau\tau} & 0 \\ 0 & R^\tau_{\tau\tau} \end{pmatrix}. \tag{5.30}$$ {?}

Lemma 4.3.2 gives

$$\rho(\sigma_2)_{ij} = (B^\tau_{\tau\tau\tau})_{ij} = \sum_f \left(\left(F^{-1}\right)^\tau_{\tau\tau\tau} \right)_{fi} R^f_{\tau\tau} \left(F^\tau_{\tau\tau\tau}\right)_{jf} \tag{5.31}$$ {?}

i.e.

$$\rho(\sigma_2) = F^{-1}RF =: B. \tag{5.32}$$ {?}

Finally, lemma 4.3.3 gives

$$\rho(\sigma_3)_{ij} = \delta_{ij} R^{\overline{j}}_{\tau\tau} \implies \rho(\sigma_3) = R_{\tau\tau} \tag{5.33}$$ {?}

since τ is its own antiparticle, $\overline{\tau} = \tau$. □

5.3.2 General braiding in $\widetilde{V}_{\tau^n}$

Recall the discussion of charge sectors from section 4.1. Since we cannot, in general, restrict the fusion space to a fixed charge sector, we shall compute the braid group generators in all charge sectors for two, three and four τ anyons. That is, we shall compute $\rho_n(\sigma_j)$ in $\widetilde{V}_{\tau^n}$ for $n = 2, 3, 4$. (This notation was introduced in definitions 4.1.1 and 4.2.1.) These examples give important insights of how the braid representation grows with the number of anyons, but most importantly these braids shall later be crucial when determining U_p in theorem 5.4.1.

ral fibonacci braiding 2⟩?

Example 5.3.4 (Braiding in $\widetilde{V}_{\tau^2}$)**.** The fusion space $\widetilde{V}_{\tau^2}$ has standard

$$\left\{ \text{valid intermediate charges } abc \text{ in } \begin{array}{c} \tau\ \tau \\ |\ \ | \\ \hline a\ b\ c \end{array} \right\} \equiv \left\{ 1\tau 1,\ 1\tau\tau,\ \tau\tau 1,\ \begin{array}{l} \tau 1\tau, \\ \tau\tau\tau \end{array} \right\}, \tag{5.34}$$

{?}

grouped into the four charge sector, 11, 1τ, $\tau 1$ and $\tau\tau$, respectively, where the first symbol denotes the left charge sector and the right symbol denotes the right charge sector.. From lemma 4.3.2 we have

$$\rho_2(\sigma_1) = B^c_{a\tau\tau} \quad \Longleftrightarrow \quad \rho_2(\sigma_1)_{ij} = (B^c_{a\tau\tau})_{ij} \tag{5.35}$$

{?}

where the indices i and j run over the given basis element. In the above given order of the basis fusion states the B-matrix is block diagonal. That is, in the obvious identification of the fusion space with $\mathbb{C}^5$ we have

$$\begin{aligned} \rho_2(\sigma_1) &= \begin{pmatrix} (B^1_{1\tau\tau})_{\tau\tau} & & & & \\ & (B^\tau_{1\tau\tau})_{\tau\tau} & & & \\ & & (B^1_{\tau\tau\tau})_{\tau\tau} & & \\ & & & (B^\tau_{\tau\tau\tau})_{11} & (B^\tau_{\tau\tau\tau})_{1\tau} \\ & & & (B^\tau_{\tau\tau\tau})_{\tau 1} & (B^\tau_{\tau\tau\tau})_{\tau\tau} \end{pmatrix} \\ &= \begin{pmatrix} R^1_{\tau\tau} & & & & \\ & R^\tau_{\tau\tau} & & & \\ & & R^\tau_{\tau\tau} & & \\ & & & B_{11} & B_{1\tau} \\ & & & B_{\tau 1} & B_{\tau\tau} \end{pmatrix} \\ &= R^1_{\tau\tau} \oplus R^\tau_{\tau\tau} \oplus R^\tau_{\tau\tau} \oplus B. \end{aligned} \tag{5.36}$$

{?}

ral fibonacci braiding 3⟩?

Example 5.3.5 (Braiding in $\widetilde{V}_{\tau^3}$)**.** Next, taking a third Fibonacci anyon τ into account gives the fusion space $\widetilde{V}_{\tau^3}$ with standard basis

$$\left\{ \begin{array}{c} \text{valid intermediate charges} \\ abcd \text{ in } \begin{array}{c} \tau\ \tau\ \tau \\ |\ \ |\ \ | \\ \hline a\ b\ c\ d \end{array} \end{array} \right\} \equiv \left\{ 1\tau\tau 1,\ \begin{array}{l} 1\tau 1\tau, \\ 1\tau\tau\tau, \end{array}\ \begin{array}{l} \tau 1\tau 1, \\ \tau\tau\tau 1, \end{array}\ \begin{array}{l} \tau 1\tau\tau, \\ \tau\tau 1\tau, \\ \tau\tau\tau\tau \end{array} \right\}. \tag{5.37}$$

{?}

Again, we have grouped the states by charge sectors. In this order of the basis we have

$$\begin{aligned} \rho_3(\sigma_1) &= R^\tau_{\tau\tau} \oplus R \oplus B \oplus \begin{pmatrix} B_{11} & & B_{12} \\ & R^\tau_{\tau\tau} & \\ B_{21} & & B_{22} \end{pmatrix} \\ \rho_3(\sigma_2) &= R^\tau_{\tau\tau} \oplus B \oplus R \oplus \begin{pmatrix} R^\tau_{\tau\tau} & & \\ & B_{11} & B_{1\tau} \\ & B_{\tau 1} & B_{\tau\tau} \end{pmatrix} \end{aligned}$$

ral fibonacci braiding 4⟩?

Example 5.3.6 (Braiding in $\widetilde{V}_{\tau^4}$)**.** In the ordered basis

$$\left\{ \begin{array}{c} \text{valid intermediate charges} \\ abcde \text{ in } \begin{array}{c} \tau\ \tau\ \tau\ \tau \\ |\ \ |\ \ |\ \ |\ \ | \\ \hline a\ b\ c\ d\ e \end{array} \end{array} \right\} \equiv \left\{ \begin{array}{l} 1\tau 1\tau 1, \\ 1\tau\tau 1\tau, \\ 1\tau\tau\tau 1, \end{array}\ \begin{array}{l} 1\tau 1\tau\tau, \\ 1\tau\tau\tau\tau, \\ 1\tau\tau\tau\tau, \end{array}\ \begin{array}{l} \tau 1\tau\tau 1, \\ \tau\tau 1\tau 1, \\ \tau\tau\tau\tau 1, \end{array}\ \begin{array}{l} \tau 1\tau 1\tau, \\ \tau 1\tau\tau\tau, \\ \tau\tau 1\tau\tau, \\ \tau\tau\tau\tau\tau \end{array} \right\} \tag{5.38}$$

{?}

we have

$$\rho_4(\sigma_1) = \begin{pmatrix} R^1_{\tau\tau} & & \\ & R^\tau_{\tau\tau} & \\ & & R^\tau_{\tau\tau} \end{pmatrix} \oplus \begin{pmatrix} B_{11} & & B_{1\tau} \\ & R^\tau_{\tau\tau} & \\ B_{\tau 1} & & B_{\tau\tau} \end{pmatrix} \oplus \begin{pmatrix} B_{11} & & & B_{12} \\ & B_{11} & & \\ & & R^\tau_{\tau\tau} & \\ B_{21} & & & B_{22} \\ & B_{21} & & \end{pmatrix} \oplus \begin{pmatrix} & & B_{12} \\ & & \\ & & \\ B_{22} & & \end{pmatrix} \tag{5.39}$$

$$\rho_4(\sigma_2) = \begin{pmatrix} B_{11} & B_{1\tau} \\ B_{\tau 1} & B_{\tau\tau} \end{pmatrix} \oplus \begin{pmatrix} B_{11} & & B_{1\tau} \\ & R^\tau_{\tau\tau} & \\ B_{\tau 1} & & B_{\tau\tau} \end{pmatrix} \oplus \begin{pmatrix} R^\tau_{\tau\tau} & & \\ & B_{11} & B_{1\tau} \\ & B_{\tau 1} & B_{\tau\tau} \end{pmatrix} \oplus \begin{pmatrix} R^1_{\tau\tau} & & & \\ & R^\tau_{\tau\tau} & & \\ & & R^\tau_{\tau\tau} & \\ & & & B_{11} & B_{12} \\ & & & B_{21} & B_{22} \end{pmatrix} \tag{5.40}$$

$$\rho_4(\sigma_3) = \begin{pmatrix} R^1_{\tau\tau} & & \\ & R^\tau_{\tau\tau} & \\ & & R^\tau_{\tau\tau} \end{pmatrix} \oplus \begin{pmatrix} R^\tau_{\tau\tau} & & \\ & B_{11} & B_{1\tau} \\ & B_{\tau 1} & B_{\tau\tau} \end{pmatrix} \oplus \begin{pmatrix} R^\tau_{\tau\tau} & & \\ & R^1_{\tau\tau} & \\ & & R^\tau_{\tau\tau} \end{pmatrix} \oplus \begin{pmatrix} B_{11} & B_{1\tau} & & \\ B_{\tau 1} & B_{\tau\tau} & & \\ & & B_{11} & B_{1\tau} \\ & & R^\tau_{\tau\tau} & \\ & & B_{\tau 1} & B_{\tau\tau} \end{pmatrix} \tag{5.41}$$

Note that in this order of the basis, the last block of $\rho_4(\sigma_2)$ is precisely $\rho_2(\sigma_1)$. Indeed, basis elements in the $\tau\tau$-sector is ordered by the internal charge sectors.

ibonacci sigma dimension⟩?

Remark 5.3.1. As is clearly manifested in the three examples, the representation of the braid group generators is always split into four blocks, one block for each two-sided charge sector, $11, 1\tau, \tau 1$ and $\tau\tau$. These blocks will always be disjoint since there is no way of transforming between them. Compare with the decomposition $V_{ab} = \bigoplus_c V^c_{ab}$. The dimension of each of these blocks grows as the Fibonacci numbers because the basis states in each block are Fibonacci strings of 1's and τ's, essentially of length $n-3, n-2, n-2, n-1$ respectively (disregarding the fixed labels due to charge sectors). Thus, by lemma 5.1.1 we have that the dimension of $\rho_n(\sigma_j)$ for n Fibonacci anyons is given by

$$\dim \rho_n(\sigma_j) = \underbrace{F_{n-1} + F_n}_{F_{n+1}} + \underbrace{F_n + F_{n+1}}_{F_{n+2}} = F_{n+3} = \dim \widetilde{V}_{\tau^n}. \tag{5.42}$$

This can be continued to compute $\rho_n(\sigma_j)$ in $\widetilde{V}_{\tau^n}$ for any n and j. This is done programmatically in appendix A.

5.3.3 Spectrum of $\rho_n(\sigma_j)$

Theorem 5.3.2. *The spectrum without multiplicities of the representation of the braid group generator $\rho_n(\sigma_j)$ is independent of n and j and given by*

$$\mathrm{spec}(\rho_n(\sigma_j)) = \left\{R^1_{\tau\tau}, R^\tau_{\tau\tau}\right\}. \tag{5.43}$$ {?}

Proof. From lemma 1.2.1 we have that the all braid group generators σ_j are conjugate, this translates to that the corresponding representations $\rho_n(\sigma_j)$ are similar for fixed n. That is, for fixed n there exists an invertible matrix S such that

$$\rho_n(\sigma_{j+1}) = S\rho_n(\sigma_j)S^{-1}. \tag{5.44}$$ {?}

(In particular we have $S = \rho_n(\sigma_j)\rho_n(\sigma_{j+1})$ from the proof of lemma 1.2.1.) Thus, the eigenvalues of $\rho_n(\sigma_j)$ are independent of j. Fix $j = 1$, the representation $\rho_n(\sigma_1)$ of σ_1 acts on $\widetilde{V}_{\tau^n}$ with basis elements

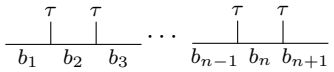

(5.45) {?}

However, only the labels b_1, b_2, b_3 enter in the expression for $\rho_n(\sigma_1)$, thus it is really only the space $\widetilde{V}_{\tau^2}$ with basis elements

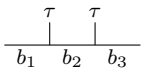

(5.46) {?}

that $\rho_n(\sigma_1)$ acts on. Thus, as discussed in remark 4.3.1, as n increases the matrix $\rho_n(\sigma_1)$ increases and gets repeated block. These repeated blocks give no new eigenvalues (but give increased multiplicity for the existing eigenvalues). Thus, the spectrum of $\rho_n(\sigma_1)$ is independent of n, not counting multiplicities.

To sum up, the spectrum of $\rho_n(\sigma_j)$, not counting multiplicities, is independent of both n and j. Thus, we can compute the spectrum from the special case $\rho_2(\sigma_1)$, computed in example 5.3.4. □

Remark 5.3.2. This theorem trivially generalizes to *any* anyon model. However, the specific eigenvalues are of course different.

5.4 Exchange operator U_p

?⟨sec:fibonacci Up⟩? Consider the fusion space $\widetilde{V}_{\tau^n}$ and exchange of a pair of anyons, j and k, around p enclosed anyons, $j+1, j+2, \ldots, k-1$. We shall use section 4.4, in particular theorem 4.4.1, to compute U_p for general p for Fibonacci anyons. As discussed in section 4.2, the dimension of the representation of the braid group depends on the number of considered anyons, in the case of Fibonacci anyons we we saw in remark 5.3.1 that the dimension of $\widetilde{V}_{\tau^n}$ increases as the Fibonacci numbers as n increases. If considering a fusion space with more particles than what enters the represented braid, the braid operator will simply get repeated block. Thus, we shall represent U_p in the fusion space $\widetilde{V}_{p+2}$. This is sufficient to compute the spectrum. Furthermore, representing U_p in a higher-dimensional fusion space is in principle straight forward and described in full generality in section 4.2.

?⟨thm:fibonacci U_p⟩? **Theorem 5.4.1.** *Exchange of a pair of τ anyons around p enclosed τ anyons introduces a non-Abelian anyonic phase U_p, given by*

$$\begin{aligned} U_0 &= \rho_2(\sigma_1) \\ U_1 &= \rho_3(\sigma_1)\rho_3(\sigma_2)\rho_3(\sigma_1) \\ U_p &= U_0^{\oplus \mathrm{Fib}(p-1)} \oplus U_1^{\oplus \mathrm{Fib}(p)}, \quad p \geq 2 \end{aligned} \tag{5.47}$$ {?}

expressed in the fused basis eq. (4.35)*, and the expression for U_p is written in a basis ordered so that all repeating blocks align nicely. The braid generators $\rho_n(\sigma_j)$ are computed in examples 5.3.4 and 5.3.5. Explicitly that is*

$$\begin{aligned} U_0 &= R^1_{\tau\tau} \oplus R^\tau_{\tau\tau} \oplus R^\tau_{\tau\tau} \oplus B \\ U_1 &= \left(R^\tau_{\tau\tau}\right)^3 \oplus (RBR) \oplus (BRB) \oplus \\ &\quad \oplus \begin{pmatrix} R^\tau_{\tau\tau}\left(B_{11}\right)^2 + B_{12}B_{21}B_{22} & B_{12}B_{21}R^\tau_{\tau\tau} & B_{12}\left(B_{22}\right)^2 + B_{11}B_{12}R^\tau_{\tau\tau} \\ B_{12}B_{21}R^\tau_{\tau\tau} & B_{11}\left(R^\tau_{\tau\tau}\right)^2 & B_{12}B_{22}R^\tau_{\tau\tau} \\ B_{21}\left(B_{22}\right)^2 + B_{11}B_{21}R^\tau_{\tau\tau} & B_{21}B_{22}R^\tau_{\tau\tau} & \left(B_{22}\right)^3 + B_{12}B_{21}R^\tau_{\tau\tau} \end{pmatrix} \end{aligned} \tag{5.48}$$ {?}

Proof. The braid corresponding to U_0 is given by theorem 4.4.1 with $c = 1$. That is, (using lemma 3.5.1)

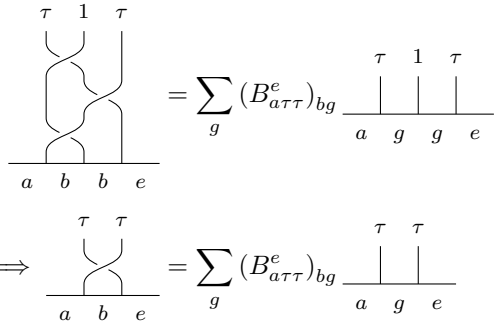

(5.49) {?}

This braid is computed as $\rho_2(\sigma_1)$ in example 5.3.4.

Similarly, the braid corresponding to U_1 is given by theorem 4.4.1 with $c = \tau$ and is computed as $\rho_3(\sigma_1)\rho_3(\sigma_2)\rho_3(\sigma_1)$ in example 5.3.5.

Finally, for $p \geq 2$ the possible values for c, i.e. the possible results from fusion of p Fibonacci anyons, are 1 and τ. Furthermore, in the fused basis eq. (4.35) the exchange operator U_p does not mix c, only the intermediate charges may be mixed when braiding. Since the two possible values for c are accounted for in U_0 and U_1, we conclude that $U_2 = U_0 \oplus U_1$. Next, lemma 5.1.2 shows that fusion of p anyons result in 1 in $\mathrm{Fib}(p-1)$ ways and τ in $\mathrm{Fib}(p)$ ways. Thus, we conclude

$$U_p = U_0^{\oplus \mathrm{Fib}(p-1)} \oplus U_1^{\oplus \mathrm{Fib}(p)}. \tag{5.50}$$ {?}

From this we have

$$\begin{aligned}\dim U_p &= \dim(U_0)\,\mathrm{Fib}(p-1) + \dim(U_1)\,\mathrm{Fib}(p)\\ &= 5\,\mathrm{Fib}(p-1) + 8\,\mathrm{Fib}(p)\\ &= 5\,(\mathrm{Fib}(p-1) + \mathrm{Fib}(p)) + 3\,\mathrm{Fib}(p)\\ &= 5\,\mathrm{Fib}(p+1) + 3\,\mathrm{Fib}(p)\\ &= 3\,\mathrm{Fib}(p+2) + 2\,\mathrm{Fib}(p+1)\\ &= 2\,\mathrm{Fib}(p+3) + \mathrm{Fib}(p+2)\\ &= \mathrm{Fib}(p+4) + \mathrm{Fib}(p+3)\\ &= \mathrm{Fib}(p+5)\end{aligned} \tag{5.51}$$ {?}

in agreement with remark 5.3.1, since $n = p + 2$.

□

Remark 5.4.1. The fact that U_p only gets repeated blocks for p for $p \geq 2$ is due to the fact that fusion of p anyons of type τ always results in 1 or τ. However, if we consider an anyon model with fusion rules

$$t \times t = a, \quad t \times a = t \tag{5.52}$$ {?}

so that

$$t \times t \times t = t \tag{5.53}$$ {?}

then U_2 and U_3 are different, since the intermediate charge c is different.

We now have an explicit expression for the exchange operator U_p, allowing us to compute the spectrum for U_p.

Corollary 5.4.2. *The eigenvalues of U_p for Fibonacci anyons are*

$$\sigma(U_p) = \left\{ \begin{array}{rll} e^{i4\pi/5} & \text{with multiplicity} & \mathrm{Fib}(p+3), \\ e^{i\pi/5} & \text{with multiplicity} & 2\,\mathrm{Fib}(p), \\ e^{-i\pi/5} & \text{with multiplicity} & 3\,\mathrm{Fib}(p), \\ e^{-i3\pi/5} & \text{with multiplicity} & 3\,\mathrm{Fib}(p-1) \end{array} \right\}. \tag{5.54}$$ {?}

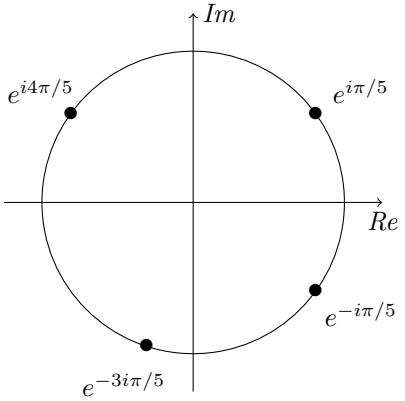

Proof. Since U_p consists of repeated block, it suffices to compute the eigenvalues for each block, multiplied by the number of occurrences for each block to get the multiplicities. Note that $B = F^{-1}RF$ is similar to R. The multiplicity for $e^{i4\pi/5}$ is $2\,\mathrm{Fib}(p-1) + 3\,\mathrm{Fib}(p) = \mathrm{Fib}(p+3)$, the other multiplicities are straight forward. □

In chapter 2 we showed the connection between eigenvalues for the exchange operator and bounds for the kinetic energy. The distance of the eigenvalues from 1 along the complex unit circle gives this energy bound. We thus see that simple exchange of two anyons has a higher corresponding kinetic energy than exchange of two anyons around $p \geq 1$ anyons. In particular U_p for $p \geq 1$ has the eigenvalue $e^{\pm i\pi/5}$ closest to 1, corresponding to kinetic energy $\lambda = 1/5$.

5.5 Quantum dimension and fusion probabilities

As discussed in detail in [12], the quantum dimension d_a of an anyon of type a is the rate of growth in dimension of the fusion space $V_{a^n}^1$ as n grows. Explicitly that is

$$d_a = \lim_{n\to\infty} \frac{\dim\left(V_{a^{n+1}}^1\right)}{\dim\left(V_{a^n}^1\right)}. \tag{5.55}$$ {?}

For Fibonacci anyons we thus have

$$d_\tau = \lim_{n\to\infty} \frac{\dim\left(V_{\tau^{n+1}}^1\right)}{\dim\left(V_{\tau^n}^1\right)} = \frac{\mathrm{Fib}(n)}{\mathrm{Fib}(n-1)} = \varphi \tag{5.56}$$ {?}

and $d_1 = 1$.

Recall from section 5.1 that fusion with a τ anyon can be represented as the matrix

$$\begin{pmatrix} 0 & 1 \\ 1 & 1 \end{pmatrix} \tag{5.57}$$ {?}

acting on

$$1 \equiv \begin{pmatrix} 1 \\ 0 \end{pmatrix}, \quad \tau \equiv \begin{pmatrix} 0 \\ 1 \end{pmatrix}. \tag{5.58}$$ {?}

Thus, fusion can be seen as a Markov process and the stationary distribution is given by the eigenvectors. The characteristic polynomial of the Fibonacci fusion matrix is

$$\begin{vmatrix} -\lambda & 1 \\ 1 & 1-\lambda \end{vmatrix} = \lambda^2 - \lambda - 1 = 0 \iff \lambda = \frac{1\pm\sqrt{5}}{2} = \varphi, -\varphi^{-1}. \tag{5.59}$$ {?}

Note the resemblance to the fusion rule, if we replace charge labels by quantum the corresponding quantum dimension,

$$\tau\times\tau = 1 + \tau \implies d_\tau^2 - d_\tau - 1 = 0 \iff d_\tau = \frac{1\pm\sqrt{5}}{2} = \varphi, -\varphi^{-1}. \tag{5.60}$$ {?}

The corresponding eigenvectors are

$$\begin{pmatrix} 1 \\ \varphi \end{pmatrix}, \quad \begin{pmatrix} 1 \\ -\varphi^{-1} \end{pmatrix} \tag{5.61}$$ {?}

which represent the steady state distribution of anyons of type 1 and τ, corresponding to the first and second component respectively, in the limit of fusion an

infinite number of times with τ anyons. The second eigenvector is non-physical, since it has a negative component. From the first eigenvector we read off the probabilities of getting 1 or τ as a result from this infinite fusion.

$$P(1) = \frac{1}{1+\varphi} = \varphi^{-2}, \quad P(\tau) = \frac{\varphi}{1+\varphi} = \varphi^{-1}. \tag{5.62}$$ {?}

That the quantum dimension $d_\tau = \varphi$ of τ is irrational illustrates the fact that the fusion space has no decomposition as a tensor product of subsystems. That is, the dimension of the fusion space does not increase by an integer factor when one more Fibonacci anyon is added, hence there is no part of the fusion space that can be factored out which describes one single particle. Indeed, if we have independent identical particles with internal Hilbert space h, then the total Hilbert space of n such particles is $\mathcal{H}_n = h^{\otimes n}$ and the quantum dimension is simply $\dim h$. Thus, quantum information encoded in the fusion space is necessarily a collective property of all anyons. Furthermore, quantum information can be encoded in the non-Abelian phase of the system, and we have seen that this anyonic phase is topological. This is the key observation motivating topological quantum computation, which we explore in the next chapter.

Chapter 6

Topological Quantum Computation

This chapter can be seen as an application of non-Abelian anyons to perform topological quantum computation. For further details see [20, 26, 28, 25].

The motivation for considering topological quantum computers is that most existing attempts at constructing quantum computers, such as ion traps, superconducting Josephson junctions and optical lattices, all share one pressing limitation; decoherence. Quantum decoherence is the effect where a quantum system, such as one implementing a quantum computer, essentially looses information to the environment. When a system is coupled to the environment, the dynamics of the system is no longer necessarily unitary, however, the total system still evolves unitarily, but it is not feasible to keep track of the exact state of the environment. The environment can introduce noise simply from heat, this eventually leads to errors in the quantum information. Efforts of completely isolating quantum systems from the environment have yet not proved successful. In some cases this can be (partially) remedied by quantum error correction algorithms.

Topological quantum computation solves the issue of decoherence by representing the quantum information in a topological state, namely the braids that we have discussed in length in previous chapters. A braid is topological in the sense that homotopy equivalent braid represent the same physical state, characterized solely by the braid group representation. There may still be an error rate, however it decreases exponentially, thus errors can effectively be removed by spatially separating the computational anyons appropriately. [26]

Abelian anyons cannot be used for quantum computation, since the fusion space of Abelian anyons is necessarily one dimensional while a qubit is two dimensional. In section 6.2 we shall see how Fibonacci anyons, as introduced in chapter 5, can be used to perform quantum computation. First we give an introduction to quantum computation in general.

6.1 Introduction to quantum computation

This section gives a concise introduction to quantum computation, defining the concepts that are built upon in topological quantum computation. The

mentioned results and further information can be found in [23].

6.1.1 Qubits

Quantum computation performs computation by manipulating qubits, similar to how classical computation performs computation by manipulating bits. A classical bit consists of exactly two discrete states, 0 and 1. A qubit is much richer, it has two orthonormal states, $|0\rangle$ and $|1\rangle$, analogous to the classical case, in addition to this a qubit can also be in linear combinations (superpositions) of these states. In other words, a qubit is a two dimensional quantum state

$$|\psi\rangle = ae^{i\alpha}|0\rangle + be^{i\beta}|1\rangle. \tag{6.1}$$ {?}

As it stands, $|\psi\rangle$ depends on four real parameters, $a \geq 0$, $b \geq 0$, α and β. However, a^2 and b^2 are the the probabilities of finding the state $|\psi\rangle$ in state $|0\rangle$ and $|1\rangle$, respectively, the superposition cannot be directly observed. This is the Born rule. Because of this, we must have $a^2 + b^2 = 1$, thus fixing one parameter $a = \sqrt{1 - b^2}$ which ranges between 0 and 1. Furthermore, the global phase of a quantum system is not physical, see section 1.3, thus an overall factor $e^{i\omega}$ is not visible and we have

$$|\psi\rangle = e^{i\omega}\left(ae^{i(\alpha-\omega)}|0\rangle + be^{i(\beta-\omega)}|1\rangle\right) \tag{6.2}$$ {?}

where ω is not known. Therefore, information of both α and β is not available, only the difference $\beta - \alpha$, as seen by eliminating ω by letting $\omega = \alpha$ so that we have

$$|\psi\rangle = e^{i\omega}\left(a|0\rangle + be^{i(\beta-\alpha)}|1\rangle\right), \tag{6.3}$$ {?}

or if we instead choose $\omega = \beta$ we put the relative phase $\alpha - \beta$ on the $|0\rangle$ state

$$|\psi\rangle = e^{i\omega}\left(ae^{i(\alpha-\beta)}|0\rangle + b|1\rangle\right). \tag{6.4}$$ {?}

In conclusion, the state $|\psi\rangle$ is determined by two real parameters, $0 \leq a \leq 1$, and $\beta - \alpha$ which is 2π periodic. Finally, note that for $a = 0$ and $a = 1$, the relative phase is no longer physical, it is part of the global phase.

6.1.2 The Bloch sphere

The space of the two parameters determining a qubit is the Cartesian product of the interval $[0, 1]$ representing the possible values for a, and the circle $[0, 2\pi]$ with endpoints 0 and 2π identified, representing the possible values for the relative phase $\beta - \alpha$. Thus we have a cylinder with the property that all points on the circles at $a = 0$ and $a = 1$, respectively, are identified, since the relative phase is non-physical at these points. The resulting space is topologically equivalent to a sphere. This space is called the Bloch sphere, see fig. 6.1. The Bloch sphere can be parametrized by spherical coordinates and every qubit state can be written uniquely as

$$|\psi\rangle = \cos(\theta/2)|0\rangle + e^{i\phi}\sin(\theta/2)|1\rangle \tag{6.5}$$ {?}

where $0 \leq \theta \leq \pi$ and $0 \leq \phi < 2\pi$. This provides geometric intuition for single-qubit operations.

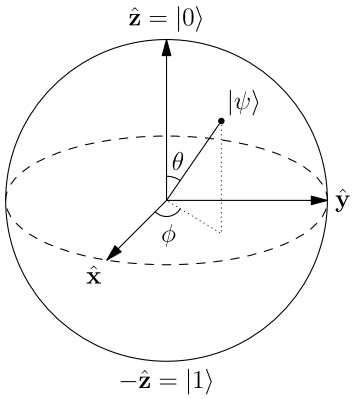

Figure 6.1: The Bloch sphere, uniquely representing all states of a qubit.

?⟨fig:bloch sphere⟩?

6.1.3 Multi-qubit systems

Similarly we can define d-dimensional analogues of qubits, referred to as qudits, by

$$|\psi\rangle = a_1 e^{i\theta_1}|0\rangle + \ldots + a_d e^{i\theta_d}|d\rangle. \tag{6.6}$$ {?}

Classically, bits are similarly generalize to computational units of d states. As in the classical case, this is not so common. To have a larger computational space we instead introduce additional qubits. The state space of a single qubit is Hilbert space $\mathcal{C}^2$, the state space of n qubits is the Hilbert space $\mathcal{H}_n = (\mathcal{C}^2)^{\otimes n} \cong \mathcal{C}^{2n}$ and the basis states are

$$|000\cdots0\rangle, |100\cdots0\rangle, |010\cdots0\rangle, |110\cdots0\rangle, |001\cdots0\rangle, \ldots, |11\cdots1\rangle, \tag{6.7}$$ {?}

where we use the notation

$$|x_1 x_2 \cdots x_n\rangle = |x_1\rangle \otimes |x_2\rangle \otimes \cdots \otimes |x_n\rangle. \tag{6.8}$$ {?}

Note the striking difference between quantum and classical bits. The state of one classical bit is determined by one number (0 or 1). The state of n classical bits is determined by n numbers (each 0 or 1), the number of parameters grows linearly. The state of one qubit is determined by two continuous parameters, the amplitude trade-off and the relative phase. The state of n qubits is determined by $2^{n+1} - 2$ continuous parameters, the term -2 is due to the fact that two parameters are fixed by normalization and the global phase. These parameters are the coefficients in the linear combination of basis states, the number of parameters grows exponentially. In conclusion, n qubits can be seen as holding exponentially more information than classical bits. However, only n classical bits can be read out from n qubits, because a measurement collapses entanglement. This is an important consideration when designing quantum algorithms.

Quantum information can be entangled across qubits. As an example, consider the case of $n = 2$ qubits, the state

$$\frac{1}{\sqrt{2}}\left(|0\rangle \otimes |1\rangle + |1\rangle \otimes |0\rangle\right) \tag{6.9}$$ {?}

is entangled, the two qubits are necessarily in opposite states. If one knows that the first qubit is in state $|0\rangle$ then the second qubit is necessarily in state $|1\rangle$, and vice versa. Both possibilities occur with probability 1/2.

6.1.4 Computing with qubits

Now, how do we actually compute with qubits? The dynamics of every quantum system is determined by the Schrödinger equation,

$$i\frac{\partial}{\partial t}|\psi(t)\rangle = H|\psi(t)\rangle \tag{6.10}$$ {?}

for some Hamiltonian H, necessarily being Hermitian and $|\psi(t)\rangle$ an element of a complex Hilbert space. The solution to this equation is

$$|\psi(t)\rangle = e^{-iHt}|\psi(0)\rangle. \tag{6.11}$$ {?}

Since every unitary matrix can be written on the form e^{-iHt}, we see that quantum states have unitary time evolution. Quantum computation is performed by taking an initial state $|\psi\rangle$, often $|\psi\rangle = |00\cdots0\rangle$, and unitarily evolving it by acting with a unitary operator U on $|\psi\rangle$ to give a new state $U|\psi\rangle$. If the system consists of n qubits, the unitary operator is an element of $U(2)^{\otimes n} = U(2^n)$, where $U(m)$ is the group of m-dimensional unitary matrices. Similarly, evolution of qudits is described by $U(d)$ matrices. Such a unitary action is achieved by appropriately manipulating the Hamiltonian H. How this happens in practice depends heavily on how the qubit system is implemented. In the case of ion traps, single qubit gates are performed by shooting a lase at the ion, and entanglement is established via electromagnetic couping. In the case of non-Abelian anyons, quantum gates are implemented via braids, as we shall see in section 6.2. Note that since unitary operators are invertible, quantum computation is necessarily reversible (provided that no wave-function collapse occurs).

6.1.5 Quantum gates and universality

c:gates and universality⟩?

Quantum gates refers to a finite set of specific unitary operators, ones that are implemented in the given physical system. Other unitary operations can then be implemented in terms of the basic quantum gates, expressed as a finite product of quantum gates. Ideally, the set of quantum gates can implement any unitary operator, if this is the case the set of quantum gates is called universal. To be precise, this is never possible since the set of unitary operators is uncountable while finite sequences of finite sets (representing products of quantum gates) is countable. Instead, universality of a set of quantum gates requires that any unitary operator can be approximated to arbitrary precision with a finite sequence of quantum gates.

Unitary operators can be interpreted as rotations in Hilbert space, single-qubit operations are effectively rotations on the Bloch sphere.

To compute the action of unitary operations one represents the basis states as the vectors

$$|0\rangle = \begin{pmatrix}1\\0\end{pmatrix}, \quad |1\rangle = \begin{pmatrix}0\\1\end{pmatrix} \tag{6.12}$$ {?}

and the tensor product (for multi-qubit systems) is computed as the Kronecker product

$$\begin{pmatrix}a\\b\end{pmatrix} \otimes \begin{pmatrix}c\\d\end{pmatrix} = \begin{pmatrix}ac\\ad\\bc\\bd\end{pmatrix}. \tag{6.13}$$ {?}

Common single-qubit gates include the Pauli operators

$$\sigma_x = \begin{pmatrix} 0 & 1 \\ 1 & 0 \end{pmatrix}, \quad \sigma_y = \begin{pmatrix} 0 & -i \\ i & 0 \end{pmatrix}, \quad \sigma_z = \begin{pmatrix} 1 & 0 \\ 0 & -1 \end{pmatrix} \tag{6.14}$$ {?}

rotating the state π radians along the x-, y- and z-axis, respectively. Note that σ_x corresponds to the classical NOT gate, flipping $|0\rangle$ and $|1\rangle$. The phase shift gate

$$R(\phi) = \begin{pmatrix} 1 & 0 \\ 0 & e^{i\phi} \end{pmatrix}; \quad |0\rangle \mapsto |0\rangle, \quad |1\rangle \mapsto e^{i\phi}|1\rangle \tag{6.15}$$ {?}

generalizes σ_z, since $R(\pi) = \sigma_z$.

None of these gates introduce superpositions, for this one can use the Hadamard gate

$$H = \frac{1}{\sqrt{2}} \begin{pmatrix} 1 & 1 \\ 1 & -1 \end{pmatrix} \tag{6.16}$$?eq:hadamard?

which maps the basis states according to

$$|0\rangle \mapsto \frac{1}{\sqrt{2}} \left(|0\rangle + |1\rangle \right), \quad |1\rangle \mapsto \frac{1}{\sqrt{2}} \left(|0\rangle - |1\rangle \right). \tag{6.17}$$ {?}

This gate has no classical counterpart.

Single-qubit cannot introduce entanglement, which is inherently a property of multiple qubit. For this, one can use the CNOT gate

$$\text{CNOT} = \begin{pmatrix} 1 & 0 & 0 & 0 \\ 0 & 1 & 0 & 0 \\ 0 & 0 & 0 & 1 \\ 0 & 0 & 1 & 0 \end{pmatrix} \tag{6.18}$$ {?}

that acts on pairs of qubits, flipping the second qubit iff the first qubit is in the state $|1\rangle$, i.e.

$$\begin{aligned} |00\rangle &\mapsto |00\rangle, \qquad |10\rangle \mapsto |11\rangle. \\ |01\rangle &\mapsto |01\rangle, \qquad |11\rangle \mapsto |10\rangle. \end{aligned} \tag{6.19}$$ {?}

It is called a controlled-NOT gate, similarly one defines the controlled-U gate for any single-qubit gate U. A fundamental result of quantum computing shows that the set $\{H, \text{CNOT}, R(\pi/4)\}$ is universal. In order have a single universal gate, it must act on at least three qubits, an example of this is the Deutsch gate $D(\theta)$ give by

$$D(\theta) = |a, b, c\rangle \mapsto \begin{cases} i\cos(\theta)|a, b, c\rangle + \sin(\theta)|a, b, 1-c\rangle & \text{for } a = b = 1 \\ |a, b, c\rangle & \text{otherwise,} \end{cases} \tag{6.20}$$ {?}

or represented as a matrix

$$D(\theta) = \begin{pmatrix} 1 & 0 & 0 & 0 & 0 & 0 & 0 & 0 \\ 0 & 1 & 0 & 0 & 0 & 0 & 0 & 0 \\ 0 & 0 & 1 & 0 & 0 & 0 & 0 & 0 \\ 0 & 0 & 0 & 1 & 0 & 0 & 0 & 0 \\ 0 & 0 & 0 & 0 & 1 & 0 & 0 & 0 \\ 0 & 0 & 0 & 0 & 0 & 1 & 0 & 0 \\ 0 & 0 & 0 & 0 & 0 & 0 & i\cos(\theta) & \sin(\theta) \\ 0 & 0 & 0 & 0 & 0 & 0 & \sin(\theta) & i\cos(\theta) \end{pmatrix}. \tag{6.21}$$ {?}

This can be seen as a controlled-controlled-$\begin{pmatrix} i\cos(\theta) & \sin(\theta) \\ \sin(\theta) & i\cos(\theta) \end{pmatrix}$ gate. It is in general a purely quantum gate, as it introduces phase shift, superposition and entanglement. In classical computing, the Toffoli gate is universal and it is precisely the $D(\pi/2)$ gate. This shows that any classical computation can be performed as a quantum computation. In fact, the other direction also holds, classical computation can simulate quantum computation. However, in general this requires an exponential increase in the number of bits.

6.1.6 Quantum algorithms

One of the most well known quantum algorithms is Shor's algorithm for integer factorization. It runs exponentially faster than the fastest known classical factoring algorithm. Time complexity is essentially determined by the number of gates needed to perform the algorithm. It is worth noting that quantum and classical gates are physically very different. Many quantum algorithms, including Shor's, gain their exponential speedup from using the n-qubit quantum Fourier transform (QFT). We wrap up this section by describing the QFT. We define the QFT on the basis states as

$$\mathcal{F}|k\rangle = \frac{1}{\sqrt{2^n}} \sum_{j=0}^{2^n-1} e^{2\pi ijk/2^n} |j\rangle \tag{6.22}$$ {?}

where we use the notation $|k_1 k_2 \cdots k_n\rangle = |k\rangle$ where k is the decimal representation of the binary string $k_1 k_2 \cdots k_n$. That is, the QFT transforms the amplitudes of a general state according to

$$\mathcal{F}\left(\sum_{k=0}^{2^n-1} x_k|k\rangle\right) = \sum_{k=0}^{2^n-1} y_k|k\rangle \tag{6.23}$$ {?}

where

$$y_k = \frac{1}{\sqrt{2^n}} \sum_{j=0}^{2^n-1} x_j e^{2\pi ijk/2^n}. \tag{6.24}$$ {?}

It is straight-forward to show that this transformation indeed is unitary. The vector $(y_k)_{k=0}^{2^n-1}$ is precisely the classical discrete Fourier transform (DFT) of the vector $(x_k)_{k=0}^{2^n-1}$. Thus, QFT on n qubits performs DFT on the 2^n complex amplitudes. This vividly illustrates the computational power of qubits. Note, however, that the entire result $(y_k)_{k=0}^{2^n-1}$ cannot be read out at once from the resulting quantum state, the amplitudes y_k can only be read off probabilistically one at a time due to the nature of quantum measurement. The full power of the QFT can be used by having the QFT as an intermediate step in a quantum algorithm.

The QFT can be decomposed as

$$\mathcal{F}|k\rangle = \frac{1}{\sqrt{2^n}} \sum_{j=0}^{2^n-1} e^{2\pi ijk/2^n} |j\rangle = \frac{1}{\sqrt{2^n}} \bigotimes_{\ell=1}^{n} \left(|0\rangle + e^{2\pi ik/2^\ell}|1\rangle\right), \tag{6.25}$$ {?}

showing that one only needs the Hadamard and phase shift gates to implement the QFT. In fact, only $n(n-1)/2$ of these gates are needed to implement the QFT, asymptotically that is $\mathcal{O}(n^2)$ number of (quantum) gates, while the classic DFT takes $\mathcal{O}(n2^n)$ number of (classical) gates.

6.2 Topological quantum computation with Fibonacci anyons

computing with fibonacci⟩? In this section we give an account based on of how topological quantum computation can be achieved with Fibonacci anyons. For further information, see [21, 27, 29, 33, 32, 31, 30].

6.2.1 Topological qubits

Implementing a qubit requires a two dimensional quantum system. Recall from chapter 5 that the fusion space $V_{\tau^4}^1$ of four Fibonacci anyons with total charge 1 is two dimensional, fewer anyons have trivial fusion spaces. We shall use the fusion space $V_{\tau^4}^1$ to model qubits. Note that $V_{\tau^4}^1 \cong V_{\tau^3}^\tau$ so we can also work with three anyons of total charge τ. In both cases no less than four Fibonacci anyons are needed, the fusion space $V_{\tau^3}^\tau$ really consists of four anyons; the fourth is the total charge. These four Fibonacci anyons can in principle be produced by pulling pairs of τ and anti-τ from the vacuum, recall that anti-τ is τ itself. This can be seen as splitting (the inverse of fusing) the vacuum $1 = \tau \times \overline{\tau} = \tau \times \tau$.

We define Fibonacci qubits by specifying the computational basis as

$$|0\rangle \coloneqq \begin{array}{c}\tau\ \tau\ \tau\ \tau \\ \hline 1\ \tau\ 1\ \tau\ 1\end{array}, \quad |1\rangle \coloneqq \begin{array}{c}\tau\ \tau\ \tau\ \tau \\ \hline 1\ \tau\ \tau\ \tau\ 1\end{array}. \tag{6.26}$$ {?}

That is, the computational basis state $|0\rangle$ is the fusion state where the first and second Fibonacci anyons fuse trivially, and computational basis state $|1\rangle$ is the fusion state where the first and second Fibonacci anyons fuse with anyonic charge τ. This also specifies how to read out data from such qubits; bring the first and second anyons close together to let them fuse and observe the resulting charge.

In the literature, in particular [21], another common notation replaces string diagrams with a special notations used specifically for Fibonacci anyons, fusion of two τ anyons is represented by

$$\begin{aligned}(\bullet,\bullet)_0 &\coloneqq \begin{array}{c}\tau\ \tau \\ \smile \\ \hline 1\end{array} = \begin{array}{c}\tau\ \tau \\ \hline 1\ \tau\ 1\end{array}, \\ (\bullet,\bullet)_1 &\coloneqq \begin{array}{c}\tau\ \tau \\ \smile \\ \hline \tau\end{array} = \begin{array}{c}\tau\ \tau \\ \hline 1\ \tau\ \tau\end{array}.\end{aligned} \tag{6.27}$$ {?}

The subscripts denote the resulting charge of the fusion and uses 0 and 1 to denote the vacuum and τ, respectively. Fusion parenthesis can be combined so that

$$((\bullet,\bullet)_{c_1},(\bullet,\bullet)_{c_2})_c = \begin{array}{c}\tau\ \tau\ \tau\ \tau \\ \smile\quad\smile \\ \hline 1\quad c_1\quad c\end{array}. \tag{6.28}$$ {?}

This is a fused state, it is not equal to a standard fusion state.

In this notation the F operator is represented as

$$(\bullet,(\bullet,\bullet)_a)_c = \sum_b F^c_{ab}\,((\bullet,\bullet)_b,\bullet)_c \tag{6.29}$$

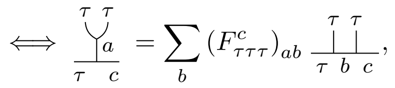

6.2.2 Single Fibonacci qubit gates

In the fusion space $V^1_{\tau^4}$ we have the braid generators

$$\rho(\sigma_1) = R, \quad \rho(\sigma_2) = B, \quad \rho(\sigma_3) = R \tag{6.30}$$

as shown in proposition 5.3.1, where

$$R = \begin{pmatrix} e^{-4\pi i/5} & 0 \\ 0 & e^{3\pi i/5} \end{pmatrix}, \quad B = \begin{pmatrix} \varphi^{-1}e^{-4\pi i/5} & \varphi e^{3\pi i/5} \\ \varphi e^{3\pi i/5} & -\varphi^{-1} \end{pmatrix} \tag{6.31}$$

and $\varphi = (1+\sqrt{5})/2$ is the golden ratio. Sometimes one works with the mirror image of this model by substituting $e^{-4\pi i/5} \mapsto e^{4\pi i/5}$ and $e^{3\pi i/5} \mapsto e^{-3\pi i/5}$, these two models are essentially the same..Thus, in this setup there are essentially four single-qubit gates, R and B and their inverses R^{-1} and B^{-1}. It is clear that the fusion space $V^\tau_{\tau^3}$ has the two braid group generators $\sigma_1 = R$ and $\sigma_2 = B$, making it clear that one can work with either one of these fusion spaces for Fibonacci qubits. Furthermore, this shows that braiding the fourth Fibonacci anyon gives nothing new, it suffices to work with σ_1 and σ_2.

As discussed in section 6.1.5, in order to be able to perform general quantum computation the set of quantum gates must be universal. The set of quantum gates $\{R, R^{-1}, B, B^{-1}\}$ for a Fibonacci qubit is indeed universal [20, 33, 26]. Thus, braiding of Fibonacci anyons is rich enough to model single qubits. However, not that the universality result only implies that there are braids that approximate any element of $SU(2)$ to arbitrary non-zero error. To achieve higher precision, longer braids are needed. It is not known if there exists a braid that exactly represents the Pauli x-matrix up to a global phase. [33, sec. 1.5]

6.2.3 Topological multi-qubit systems

In order to perform general quantum computation we must be able to manipulate multiple qubits. The Hilbert space $\mathcal{H}_n$ of n qubits is 2^n dimensional, therefore we must have a fusion space of at least 2^n dimensions in order to model $\mathcal{H}_n$. We shall not expect to find fusion spaces of exactly 2^n dimensions since the dimension of the fusion space $V^1_{\tau^m}$ of m Fibonacci anyons grow as the Fibonacci numbers with increasing m.

In order to implement two qubits, a fusion space of at least dimension four shall be needed. The smallest fusion space $V^1_{\tau^m}$ with dimension at least four is

$$V^1_{\tau^6} = \mathrm{span}\{\ldots\} \tag{6.32}$$

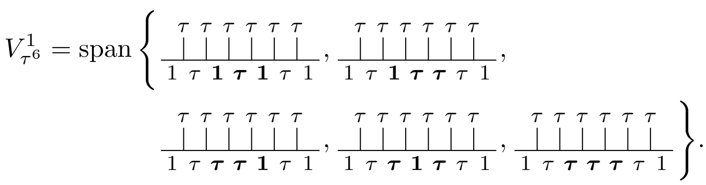

In principle one can declare the computational basis states $|00\rangle, |01\rangle, |10\rangle, |11\rangle$ to be the first through forth fusion states, leaving the fifth fusion state non-computational. A more efficient scheme would be to let each of these fusion states be one of the states of a five dimensional qudit. More generally, the fusion space $V_{\tau^n}^1$, which is $\mathrm{Fib}(n-1)$ dimensional, can be used to implement a $\mathrm{Fib}(n-1)$ dimensional qudit.

The most common approach in the literature instead uses n Fibonacci qubits to implement n qubits, by using the fusion space $V_{\tau^{2n+2}}^1$. The computational basis is defined as

$$|x_1 x_2, \dots x_n\rangle \coloneqq \tau\ \tau\ \tau\ \tau\ \tau \quad \tau \\ 1\ \tau\ a_{x_1}\ \tau\ a_{x2}\ \tau \cdots \tau\ 1 \tag{6.33}$$ {?}

where $a_0 = 1$ and $a_1 = \tau$.

The quantum gates of this system is exactly the possible braids, generated by the braid generators $\rho_m(\sigma_j)$, as computed in general in chapter 5 and appendix A. Similar to single Fibonacci qubits, also multi-Fibonacci-qubits gates are universal [33]. However, efficiently finding braids that approximate a given unitary operator can be difficult, a brute force search becomes infeasible as the dimension of the Hilbert space increases, because number of possible braids braids increases exponentially. A solution to this is the Solovay-Kitaev theorem, one of the fundamental results in quantum computing. The theorem essentially states that give a set universal gates, there is a method for approximating any gate with a surprisingly short sequence of gates [23, Appendix 3] [24]. This method has been successfully applied to Fibonacci qubits in, for example, [21] to efficiently find braids that approximate any unitary operation.

6.2.4 Leakage errors

For $n \geq 2$, the fusion space $V_{\tau^{2n+2}}^1$ has higher dimension than the number of computational states, indeed $\mathrm{Fib}(2n+1) > 2^n$. This leads to the existence of non-computational fusion states. During braiding, this can lead to errors known as leakage errors. To clearly see this, consider $n = 2$ Fibonacci qubits, i.e. the fusion space $V_{\tau^{2n+2}}^1 = V_{\tau^6}^1$, the computational basis is

$$\begin{aligned}
|00\rangle &= \tau\ \tau\ \tau\ \tau\ \tau\ \tau \\ 1\ \tau\ \mathbf{1}\ \tau\ \mathbf{1}\ \tau\ 1 \\
|01\rangle &= \tau\ \tau\ \tau\ \tau\ \tau\ \tau \\ 1\ \tau\ \boldsymbol{\tau}\ \tau\ \mathbf{1}\ \tau\ 1 \\
|10\rangle &= \tau\ \tau\ \tau\ \tau\ \tau\ \tau \\ 1\ \tau\ \mathbf{1}\ \tau\ \boldsymbol{\tau}\ \tau\ 1 \\
|11\rangle &= \tau\ \tau\ \tau\ \tau\ \tau\ \tau \\ 1\ \tau\ \boldsymbol{\tau}\ \tau\ \boldsymbol{\tau}\ \tau\ 1 \\
|NC\rangle &= \tau\ \tau\ \tau\ \tau\ \tau\ \tau \\ 1\ \tau\ \boldsymbol{\tau}\ \mathbf{1}\ \boldsymbol{\tau}\ \tau\ 1
\end{aligned} \tag{6.34}$$ {?}

where $|NC\rangle$ denotes the non-computational state. Generally there are several non-computational states, but only one in this example. When performing

braiding, even though the computation starts out in a computational state, a braid may take the state to a non-computational state. A clear example of this is braiding of the third and fourth Fibonacci anyon when in the $|11\rangle$ state, this takes the state to a superposition of $|11\rangle$ and $|NC\rangle$ according to

$$B : \begin{array}{c}\tau\ \tau\\ |\ |\\ \hline \tau\ \tau\ \tau\end{array} \mapsto \begin{array}{c}\tau\ \tau\\ \smile\\ \hline \tau\ \tau\ \tau\end{array} = (B^{\tau}_{\tau\tau\tau})_{1\tau} \begin{array}{c}\tau\ \tau\\ |\ |\\ \hline \tau\ 1\ \tau\end{array} + (B^{\tau}_{\tau\tau\tau})_{\tau\tau} \begin{array}{c}\tau\ \tau\\ |\ |\\ \hline \tau\ \tau\ \tau\end{array}. \tag{6.35}$$ {?}

The problem of leakage errors becomes unavoidable when performing braids that entangle two qubit. Entangling qubits is needed in order to perform general quantum computation, this can be done by braiding the Fibonacci anyons of the first qubit around the Fibonacci anyons, this necessarily introduces leakage errors. In [21, 22] various methods to work around this is discussed. It is shown that transitions into the non-computational state can be tracked and avoided by braiding only one Fibonacci anyon while keeping all other fixed, called single particle weaves. This scheme still allows for universal quantum computation. To illustrate how this works, consider the first qubit and the corresponding non-computational state,

$$\begin{aligned} |0\rangle &= \begin{array}{c}\tau\ \tau\ \tau\\ |\ |\ |\\ \hline 1\ \tau\ 1\ \tau\end{array}\\ |1\rangle &= \begin{array}{c}\tau\ \tau\ \tau\\ |\ |\ |\\ \hline 1\ \tau\ \tau\ \tau\end{array}\\ |NC\rangle &= \begin{array}{c}\tau\ \tau\ \tau\\ |\ |\ |\\ \hline 1\ \tau\ \tau\ 1\end{array}. \end{aligned} \tag{6.36}$$ {?}

The corresponding braid group generators are

$$\begin{aligned} \rho(\sigma_1) &= \begin{pmatrix} e^{i4\pi/5} & 0 & 0\\ 0 & e^{-i3\pi/5} & 0\\ 0 & 0 & e^{-i3\pi/5}\end{pmatrix}\\ &= \begin{pmatrix} e^{i4\pi/5} & 0\\ 0 & e^{-i3\pi/5}\end{pmatrix} \oplus e^{-i3\pi/5}\\ \rho(\sigma_2) &= \begin{pmatrix} \varphi^{-1}e^{-4\pi i/5} & \varphi e^{3\pi i/5} & 0\\ \varphi e^{3\pi i/5} & -\varphi^{-1} & 0\\ 0 & 0 & e^{-3i\pi/5}\end{pmatrix}\\ &= \begin{pmatrix} \varphi^{-1}e^{-4\pi i/5} & \varphi e^{3\pi i/5}\\ \varphi e^{3\pi i/5} & -\varphi^{-1}\end{pmatrix} \oplus e^{-i3\pi/5}. \end{aligned} \tag{6.37}$$ {?}

Note that [21] uses the mirrored phase convention. In this way, any braid accumulates a phase $e^{-i3W\pi/5}$ in the non-computational block, where W is the winding number of the braid. Thus, the winding number can be used to put restrictions on braids and avoid transitions into the non-computational state.

Appendix A

Programmatically computing $\rho_n(\sigma_j)$ for Fibonacci anyons

?⟨sec:code⟩? In this appendix we compute the representation for the braid group generators $\rho_n(\sigma_j)$ in $\widetilde{V}_{\tau^n}$, for any $2 \geq n$ and $1 \geq j \geq n-1$.

A.1 Symbolic computation

The following Mathematica code symbolically generates $\rho_n(\sigma_j)$ for any n and j.

```
(* FibString[n] returns a list all Fibonacci strings
   of length n, sorted by charge sectors.
   A Fibonacci string is a list of 1's and 2's with no recurring 1's. *)

FibStringRecurse[1] := {{1}, {2}};
FibStringRecurse[n_] := Flatten[
    Map[
        If[
            Last[#] == 2,
            {Flatten[{#, 1}],
            Flatten[{#, 2}]}, {Flatten[{#, 2}]}
        ] &,
        FibString[n - 1]],
    1
];

FibString[n_] := SortBy[FibStringRecurse[n], {First[#], Last[#]} &];

(* FibStringCS[n, csl, csr] returns FibString[n] restricted to left and right
   charge sectors given by csl and csr. *)
FibStringCS[n_, csl_, csr_] := Select[
    FibStringRecurse[n],
    First[#] == csl && Last[#] == csr &
```

```
];

(* σ[n,j] returns the representation of the j:th braid group generator
   in the fusion space of n Fibonacci anyons, including all possible
   left and right charge sectors. *)
σMeta[n_, j_, fusionStates_] := Map[
    Module[{labels, row, idx, idx2, fusionStateCopy},
        fusionStateCopy = #;
        labels = Take[#, {j, j + 2}];
        row = ConstantArray[0, Length[fusionStates]];
        idx = Position[fusionStates, #][[1]][[1]];
        Switch[labels,
            {1, 2, 1}, row[[idx]] = R1,
            {1, 2, 2}, row[[idx]] = Rτ,
            {2, 2, 1}, row[[idx]] = Rτ,
            {2, 1, 2}, (
                row[[idx]] = B11;
                fusionStateCopy[[j + 1]] = 2;
                idx2 = Position[fusionStates, fusionStateCopy][[1]][[1]];
                row[[idx2]] = B12
            ),
            {2, 2, 2}, (
                row[[idx]] = B22;
                fusionStateCopy[[j + 1]] = 1;
                idx2 = Position[fusionStates, fusionStateCopy][[1]][[1]];
                row[[idx2]] = B21;
            )
        ];
        row
    ] &, fusionStates];

σ[n_, j_] := σMeta[n, j, FibString[n + 1]];

σ[n_, j_, csl_, csr_] := σMeta[n, j, FibStringCS[n + 1, csl, csr]];

(* U[p] returns σ₁σ₂⋯σₚσₚ₊₁σₚ⋯σ₂σ₁ on p+2 Fibonacci anyons. *)
U[p_] := Dot @@ Flatten[{
    Table[σ[p + 2, j], {j, 1, p + 1}],
    Table[σ[p + 2, j], {j, p, 1, -1}]
}, 1];
U[p_, csl_, csr_] := Dot @@ Flatten[{
    Table[σ[p + 2, j, csl, csr], {j, 1, p + 1}],
    Table[σ[p + 2, j, csl, csr], {j, p, 1, -1}]
}, 1];

(* Example *)
Print[MatrixForm[σ[3, 1]]];
Print[σ[3, 1].σ[3, 2].σ[3, 1] == U[1]];
```

A.2 Numeric computation

The following code builds on the code in the previous section to give numerical values for the braid group generators.

```
(* Plug in values for the parameters. *)
R1 = Exp[4 Pi I/5];
Rτ = Exp[-3 Pi I/5];
R = ({
    {R1, 0},
    {0,  Rτ}
});
φ = GoldenRatio;
F = ({
    {φ^-1,      φ^(-1/2)},
    {φ^(-1/2), -φ^-1}
});
B = Inverse[F].R.F;
B11 = B[[1, 1]];
B12 = B[[1, 2]];
B21 = B[[2, 1]];
B22 = B[[2, 2]];

(* Compute argument of eigenvalues. Performance boos by computing using N[..],
   then convert back by Rationalize[../Pi]. *)
EigenvaluesArg[data_] := Sort[Rationalize[Arg[Eigenvalues[N[data]]]/Pi]Pi];

(* Example *)
Print[EigenvaluesArg[σ[3, 1]]];
```

Bibliography

nakahara [1] Nakahara: Geometry, Topology and Physics. En trevlig och koncis introduktion till homotopi-grupper finns i kap 4, kap 2-3 kan dock behövas som förkunskaper. Denna bok har tidigare funnits på kårbokhandeln och tycker jag är helt klart värd att investera i, annars kolla biblioteket eller kontakta mig. Observera att man kan hoppa över kap 1 för matematiken.

wilczek [2] F. Wilczek. *Quantum Mechanics of Fractional-Spin Particles.* Physical Review Letters. 49 (14): 957–959. Bibcode:1982PhRvL..49..957W. doi:10.1103/PhysRevLett.49.957. (1982)

?lundholm-solovej? [3] D. Lundholm, J. Solovej. *Hardy and Lieb-Thirring Inequalities for Anyons.* arXiv:1108.5129, http://dx.doi.org/10.1007/s00220-013-1748-4, Matematisk bakgrund samt exklusionsprincip för abelska anyoner.

?mancarella? [4] F. Mancarella, A. Trombetoni. *Statistical Mechanics of an Ideal Gas of Non-Abelian Anyons.* arXiv:1204.6656

fröhlich [5] J. Fröhlich. *Quantum statistics and locality.* Proceedings of the Gibbs symposium, Yale University, May 15-17 (1989)

?myrheim? [6] L. Myrheim. *Anyons.*

oskar [7] O. Weinberger. *The braid group, representations and non-abelian anyons.* Bachelor's thesis, KTH

configuration spaces [8] E. Fadell, L. Neuwirth. *Configuration spaces.* Math. Scand. 10 (1962) 111–118

feynmann path integral [9] R. P. Feynman. *Space-time approach to non-relativistic quantum mechanics.* Rev. Mod. Phys. 20 (1948) 367–387.

distinguishable particles [10] M. G. G. Laidlaw, C. M. DeWitt. *Feynman functional integrals for systems of indistinguishable particles.* Phys. Rev. D 3 (1971) 1375–1378.

kitaev [11] A. Kitaev. *Anyons in an exactly solved model and beyond.* Annals of Physics 321 (2006) 2. (Revised version arXiv:cond-mat/0506438.)
(One of the founding papers. See especially Appendix E.)

preskill [12] J. Preskill. *Lecture Notes for Physics 219: Quantum Computation, Chapter 9: Topological quantum computation.*
http://www.theory.caltech.edu/~preskill/ph219/topological.pdf

bonderson [13] P. H. Bonderson *Non-Abelian Anyons and Interferometry.* (2007) Ph.D Thesis

short intro fib [14] S. Trebst, M. Troyer, Z. Wang and A. W. W. Ludwig. *A Short Introduction to Fibonacci Anyon Models.* Progress of Theoretical Physics Supplement No. 176, 2008.
http://stationq.cnsi.ucsb.edu/~wang/Publications/34.pdf

mac lane [15] S. Mac Lane. *Categories for the Working Mathematician, 2nd Edition.* Graduate Texts in Mathematics, Springer-Verlag (1998).

tuba [16] I. Tuba. *Braid Representations and Tensor Categories.* PhD thesis, University of California.

naaijkens [17] P. Naaijkens. *PhD Thesis: Anyons in Infinite Quantum Systems: QFT in* $d = 2 + 1$ *and the Toric Code* http://www.math.ru.nl/~landsman/Naaijkens.pdf
(Contains an account of the categorical framework for anyons.)

prakash [18] P Panangaden, E. Paquette *A categorical presentation of quantum computation with anyons.*
http://www.cs.mcgill.ca/~prakash/Pubs/MTCanyons.pdf

tensor categories [19] Etingof, Gelaki, Nikshych, Ostrik. *Tensor Categories.* AMS http://www-math.mit.edu/~etingof/egnobookfinal.pdf

nayak [20] C. Nayak, S. H. Simon, A. Stern, M. Freedman, S. D. Sarma. *Non-Abelian Anyons and Topological Quantum Computation.* arXiv:0707.1889

ological quantum compiling [21] L. Hormozi, G. Zikos, N. Bonesteel, S. Simon. *Topological quantum compiling.* Phys. Rev. B 75, 165310 (2007), arXiv:quant-ph/0610111
http://link.aps.org/doi/10.1103/PhysRevB.75.165310

one mobile quasiparticle [22] S. Simon, N. Bonesteel, M. Freedman, N. Petrovic, L. Hormozi. *Topological Quantum Computing with Only One Mobile Quasiparticle.* arXiv:quant-ph/0509175

nielsen chuang [23] M. Nielsen, I. Chuang. *Quantum computation and quantum information.* Cambridge university press (2010).

dawson nielsen [24] C. Dawson, M. Nielsen. *The Solovay-Kitaev algorithm.* arXiv:quant-ph/0505030

braid topologies [25] N. Bonesteel, L. Hormozi, G. Zikos, and S. Simon. *Braid topologies for quantum computation.* Phys. Rev. Lett. 95 (2005), 140503. arXiv:quant-ph/0505665.

reedman kitaev larsen wang [26] M. Freedman, A. Kitaev, M. Larsen and Z. Wang. *Topological quantum computation.* Bull. Am. Math. Soc. 40 (2003), p. 31–38.
http://dx.doi.org/10.1090/S0273-0979-02-00964-3

taev fault-tolerant anyons [27] A. Kitaev. *Fault-tolerant quantum computation by anyons.* arXiv:quant-ph/9707021

shor fault-tolerant [28] P. Shor. *Fault-tolerant quantum computation.* arXiv:quant-ph/9605011

kauffman lomonaco [29] L. H. Kauffman, S. J. Lomonaco. *Topological quantum computing and $SU(2)$ braid group representations.* Proc. of SPIE Vol. 6976 69760M-1 (2008)

slingerland bais [30] J.K. Slingerland, F.A. Bais. *Quantum groups and nonabelian braiding in quantum Hall systems* arXiv:cond-mat/0104035

asymptotical top compl [31] V. Kliuchnikov, A. Bocharov, K. Svore. *Asymptotically optimal topological quantum compiling.*
arXiv:1310.4150

pachos book [32] J. Pachos. *Introduction to Topological Quantum Computation.* Cambridge University Press.
http://quantum.leeds.ac.uk/jiannis-pachos/book.html
http://quantum.leeds.ac.uk/fileadmin/user_upload/Jiannis/IntroTQC.pdf

wang book [33] Z. Wang. *Topological Quantum Computation.* Microsoft Research Station Q, University of California. AMS and CBMS. http://www.math.ucsb.edu/~zhenghwa/data/course/cbms.pdf

?lundholm-rougerie? [34] D. Lundholm, N. Rougerie. *Emergence of Fractional Statistics for Tracer Particles in a Laughlin Liquid.* PRL 116, 170401 (2016)

abelian fqh [35] F. Camino, Z. Wei, V. Goldman. *Realization of a Laughlin quasiparticle interferometer: Observation of fractional statistics.* Physical Review B. 72 (7). arXiv:cond-mat/0502406.

non-abelian experimental [36] S. An, P. Jiang, H. Choi, W. Kang, S. Simon, L. Pfeiffer, K. West, K. Baldwin. *Braiding of Abelian and Non-Abelian Anyons in the Fractional Quantum Hall Effect.* arXiv:1112.3400